



Published in final edited form as:

Nature. 2016 July 7; 535(7610): 164–168. doi:10.1038/nature18625.

A CRISPR screen defines a signal peptide processing pathway required by flaviviruses

Rong Zhang¹, Jonathan J. Miner¹, Matthew J. Gorman¹, Keiko Rausch⁵, Holly Ramage⁵, James P. White¹, Adam Zuiani¹, Ping Zhang^{1,6}, Estefania Fernandez¹, Qiang Zhang¹, Kimberly A. Dowd⁷, Theodore C. Pierson⁷, Sara Cherry⁵, and Michael S. Diamond^{1,2,3,4,*}

¹Department of Medicine, Washington University School of Medicine, Saint Louis, MO 63110 USA

²Department of Molecular Microbiology, Washington University School of Medicine, Saint Louis, MO 63110 USA

³Department of Pathology and Immunology, Washington University School of Medicine, Saint Louis, MO 63110 USA

⁴The Center for Human Immunology and Immunotherapy Programs, Washington University School of Medicine, Saint Louis, MO 63110 USA

⁵Department of Microbiology, Perelman School of Medicine, University of Pennsylvania, Philadelphia, PA, 19104 USA

⁶Department of Immunology, Institute of Human Virology, Zhongshan School of Medicine, Sun Yat-sen University, Guangzhou 510080, China

⁷Viral Pathogenesis Section, National Institute of Allergy and Infectious Diseases, National Institutes of Health, Bethesda, MD 20892 USA

Abstract

Flaviviruses infect hundreds of millions of people annually, with no antiviral therapy available^{1,2}.

We performed a genome-wide CRISPR/Cas9-based screen to identify host genes that when edited resulted in reduced flavivirus infection. We validated nine human genes required for flavivirus infectivity, and these were associated with endoplasmic reticulum (ER) functions including translocation, protein degradation, and N-linked glycosylation. In particular, a subset of ER-

Users may view, print, copy, and download text and data-mine the content in such documents, for the purposes of academic research, subject always to the full Conditions of use:http://www.nature.com/authors/editorial_policies/license.html#terms

*Address correspondence to: Michael S. Diamond, M.D. Ph.D., Departments of Medicine, Molecular Microbiology, and Pathology and Immunology, Washington University School of Medicine, 660 South Euclid Ave. Box 8051, Saint Louis, MO 63110, USA. diamond@borcim.wustl.edu, (314) 362-2842.

AUTHOR CONTRIBUTIONS

R.Z. performed the primary CRISPR/Cas9 screen and viral protein transfection experiments. Validation studies in cells with different viruses were performed by R.Z., P.Z., M.J.G, A.Z., E.F., and M.S.D. J.J.M. performed the pulse-chase experiments and mass cytometry. J.P.W. performed studies with replicons. K.R. and H.R. performed the insect cell and insect experiments. Q.Z. performed the secretome analysis and mass spectrometry. R.Z., S.C., T.C.P., and M.S.D. designed the experiments. K.A.D. and T.C.P. provided key reagents. Q.Z. performed data analysis. S.C. and M.S.D. wrote the initial draft of the manuscript, with the other authors contributing to editing into the final form.

COMPETING FINANCIAL INTERESTS

The authors have no financial conflicts to disclose.

associated signal peptidase complex (SPCS) proteins was necessary for the proper cleavage of the flavivirus structural proteins (prM and E) and secretion of viral particles. Loss of SPCS1 expression resulted in markedly reduced yield of all *Flaviviridae* family members tested (West Nile, Dengue, Zika, yellow fever, Japanese encephalitis, and hepatitis C viruses), yet had little impact on alphavirus, bunyavirus, or rhabdovirus infection or the surface expression or secretion of diverse host proteins. We found that SPCS1 dependence could be bypassed by replacing the native prM protein leader sequences with a class I MHC antigen leader sequence. Thus, SPCS1, either directly or indirectly via its interactions with unknown host proteins, preferentially promotes the processing of specific protein cargo, and *Flaviviridae* have a unique dependence on this signal peptide processing pathway. SPCS1 and other signal processing pathway members could represent pharmacological targets for inhibiting infection of the expanding number of flaviviruses of medical concern.

We performed a genome-wide inhibition of West Nile virus (WNV)-induced cell death screen using the CRISPR/Cas9 system³⁻⁷ and lentiviruses targeting 19,050 genes (Extended Data Fig 1a). Whereas in the absence of lentivirus transduction, cells did not survive WNV infection, colonies of lentivirus-transduced cells survived; sgRNAs were amplified by PCR, and sequenced. We identified 12 genes that statistically were enriched using MAGeCK⁸ (Supplementary Tables 1 and 2). All 12 genes were ER-associated with annotated functions of carbohydrate modification, protein translocation and signal peptide processing, protein degradation, and heat shock response (Fig 1a).

In validation studies, editing of nine genes resulted in reduced WNV antigen expression following infection of 293T or HeLa cells (Fig 1a–b) without causing cytotoxicity (Extended Data Fig 1b). We confirmed the efficiency of gene editing for the proteins for which we could obtain validated antibodies (Extended Data Fig 1c). Validated genes were tested for effects on related flaviviruses: Zika (ZIKV), Japanese encephalitis (JEV), Dengue serotype 2 (DENV-2), and yellow fever (YFV) viruses. Editing of six of these genes reduced infection of all four flaviviruses (Fig 1c–f). Editing of *STT3A*, *SEC63*, *SPCS1*, or *SPCS3* resulted in decreased yields of WNV and JEV (Fig 1g–h). We observed less impact on unrelated positive- or negative-sense RNA viruses (Extended Data Fig 1d).

As pathogenic flaviviruses are arthropod-transmitted, we evaluated the roles of orthologs in insect cells. Silencing of *Drosophila* orthologs reduced infection of WNV and DENV-2 (Fig 2a–b) without appreciably affecting cell viability (Fig 2c). Decreased WNV infection also was observed in mosquito cells after silencing (Fig 2d). Depletion of *dSPASE22-23* [*SPCS3*] in adult flies led to decreased WNV titers (Fig 2e) and flies heterozygous for *dSPASE12* [*SPCS1*] showed reduced WNV infection (Fig 2f). Altogether, flavivirus infectivity in human and insect cells was dependent on analogous ER-associated genes.

Trans-complementation of gene-edited human cells with wild-type alleles rescued flavivirus infectivity (Extended Data Fig 1e–g). Since we identified two (SPCS1 and SPCS3) of the five components of the Signal Peptidase Complex^{9,10}, and found that insect SPCS genes also affected flavivirus infection, we focused study on these genes. Gene silencing in human cells confirmed that SPCS genes were required for optimal flavivirus but not alphavirus infection (Extended Data Fig 2 and data not shown).

We screened for clonal SPCS1 and SPCS3 KO cells lines. Although we were unable to obtain SPCS3^{-/-} clonal lines, SPCS1^{-/-} 293T or Huh7.5 cell clones grew, with both alleles containing nonsense deletions (Fig 3a and Extended Data Fig 3). WNV, DENV, JEV, YFV, and ZIKV failed to accumulate in the supernatants of SPCS1^{-/-} 293T cells (Fig 3c–f), and the WNV phenotype was restored in trans-complemented cells (Fig 3h). However, SPCS1^{-/-} cells supported infection of alphaviruses, bunyaviruses, and rhabdoviruses (Fig 3i–k, and Extended Data Fig 3a). To corroborate these findings, we measured infection in SPCS1^{-/-} Huh7.5 cells and showed reduced infection of WNV, ZIKV, JEV, and also of the related *Flaviviridae* member, hepatitis C virus (Extended Data Fig 3e–f). In comparison, gene editing of the remaining SPCS proteins, SEC11A and SEC11C, had minimal effects on infection (Extended Data Fig 4).

To determine whether SPCS1 was required for viral translation and/or replication, we utilized WT and loss-of-function¹¹ flavivirus replicons encoding reporter genes¹² (Fig 3b and Extended Data Fig 5). Transfection of control cells with replicon RNA resulted in low levels of reporter gene activity over the first several hours, which reflects translation of input viral RNA, whereas subsequent signal increases are due to RNA replication. In SPCS1^{-/-} cells, high levels of reporter gene expression were observed, indicating that viral RNA translation and replication remained largely intact.

We speculated that SPCS subunits, directly or indirectly, might regulate cleavage of the flavivirus polyprotein¹³. Flavivirus structural (prM and E), and non-structural (NS1 and NS4B) proteins are cleaved by unknown ER host signal peptidase(s) (Fig 3l and^{14,15}). Gene-edited 293T cells were infected with WNV or JEV, and lysates were analyzed. Reduced levels of E and prM proteins were present in SPCS1^{-/-} clones and SPCS1 or SPCS3 bulk gene-edited cells at 12 h, and by 24 h higher molecular weight bands reacted with anti-E or -prM/E antibodies¹⁶ (Fig 3m–n and Extended Data Figs 3g and 6a–b). We next examined the requirement for SPCS1 on cleavage of NS1-NS2A, 2K-NS4B, and NS2B-NS3. In SPCS1^{-/-} cells, infection with WNV resulted in decreased expression of NS1 and the accumulation of higher molecular weight bands (Fig 3o). For NS4B, we detected lower levels of protein in SPCS1^{-/-} cells; in transfection studies with a tagged 2K-NS4B plasmid, a higher molecular weight band was observed. For NS1-NS2A and NS3, we did not detect aberrant cleavage (Extended Data Fig 6). We also tested the effects on HCV E2 glycoprotein and found decreased levels in SPCS1-deficient cells (Extended Data Fig 7). In comparison, alphavirus or bunyavirus glycoproteins, which also require ER processing^{17,18}, had intact expression in SPCS1-deficient cells (Fig 3p and Extended Data Fig 3b–c).

To isolate the effects of the SPCS complex from infection, we transfected a prM-E plasmid, which produces subviral particles (SVPs)¹⁹. Immunoblotting of cell lysates for E and prM proteins showed reduced levels and higher molecular weight bands in SPCS1 or SPCS3 deficient cells, which correlated with fewer SVPs (Extended Data Fig 8a–c). We tested if there was a dependency of SPCS1 for cleavage of flavivirus protein signal sequences. We transfected WNV structural (capsid (C), prM/M, E) and secreted (NS1) genes with native or MHC class I (K^b) signal sequences into SPCS1^{-/-} cells, and evaluated effects on expression (Fig 4).

Expression of C protein from a C-prM-E plasmid was equivalent in control and SPCS1^{-/-} cells, although in the absence of the viral protease, C did not migrate at its normal size (Extended Data Fig 8d). Cleavage of the downstream proteins prM and E was reduced in SPCS1^{-/-} cells, as some of the C protein migrated aberrantly. When NS2B-NS3 was supplied *in trans*, C was cleaved from prM-E and accumulated at the correct size in control and SPCS1^{-/-} cells. Thus, expression or cleavage of C is not affected by SPCS1.

We next evaluated prM/M expression. When the native prM leader sequence was used, expression of prM and its furin-cleavage product M was reduced in SPCS1^{-/-} cells (Fig 4a, *groups 1 and 3*). Substitution of the K^b leader rescued prM/M expression in SPCS1^{-/-} cells only when prM was on a separate plasmid (Fig 4a, *group 2*) but not as a prM-E plasmid (Fig 4a, *group 4*). Thus, specific leader sequences determine the dependence of prM/M protein expression on SPCS1, and downstream proteins can modulate processing efficiency.

When E was transfected, its expression was largely independent of SPCS1 or transplantation of the K^b leader sequence (Fig 4b, *groups 1 and 2*). When E was cloned downstream of prM, accumulation of E was not detected in SPCS1^{-/-} cells (Fig 4b, *groups 3 and 4*). This suggested that the native leader sequence of E was not cleaved in SPCS1^{-/-} cells when presented as an “internal” leader sequence or epistatic effects of the upstream prM protein inhibited E protein stability. To evaluate this question, we performed ³⁵S pulse-chase studies in prM-E transfected cells. In control cells, only a single E protein band was visible indicating rapid prM-E cleavage. However, prM-E and E bands both were present in SPCS1^{-/-} cells (Fig 4c, *top*) and remained in an ER-resident form (Fig 4c, *bottom*). A short 3-minute ³⁵S pulse showed a delay in the cleavage of prM-E in SPCS1^{-/-} cells (Fig 4d).

We assessed expression of NS1, which also requires ER-dependent signal sequence cleavage. When NS1 was transfected, SPCS1 was dispensable for expression (Fig 4e, *group 1*). When cloned downstream of E (Fig 4e, *groups 2 and 3*) or prM-E (Fig 4e, *groups 4 and 5*), NS1 levels were reduced in SPCS1^{-/-} cells. After blotting with anti-NS1 MAb, a 90 kDa weight band was visible in SPCS1^{-/-} cells (Fig 4e, *group 2*), which likely represented uncleaved E-NS1; this result was corroborated by blotting for E protein (Fig 4b, *groups 5 and 6*). Thus, placement of the NS1 leader sequence into an internal position rendered it more dependent on SPCS1 for cleavage.

Flavivirus SVPs can be produced after transfection of prM and E on single or separate plasmids^{20,21}. Transfection of prM-E encoding native or K^b and native internal signal sequences resulted in loss of expression of prM and E or SVPs in SPCS1^{-/-} cells (Fig 4f, *groups 5 and 6*). When prM and E were co-transfected, protein was detected in SPCS1^{-/-} cell lysates (Fig 4f, *groups 1 and 2*) and supernatant, albeit at lower levels. In SPCS1^{-/-} cells, prM negatively affected E but not NS1 production (Fig 4f, compare *groups 1, 2, and 7* and Extended Data Fig 8e), possibly because of its chaperone-like function for E²⁰. Defects in prM and E co-expression in SPCS1^{-/-} cells were corrected by inserting the K^b leader sequence in front of the prM gene (Fig 4f, *groups 3 and 4*). A 3-minute ³⁵S pulse and immunoprecipitation experiment in SPCS1^{-/-} cells showed an uncleaved form of prM (Fig 4g).

To assess whether host surface proteins might require SPCS1 for signal peptide processing we profiled SPCS1^{-/-} Jurkat T cells. Whereas ten antigens showed no difference in surface expression, levels of CD49d/CD29, ULBP1, and HLA-E were reduced 2 to 3-fold (Extended Data Figure 9a–c). A decrease in surface expression of ULBP1 was reported in cells deficient in SPCS1 or SPCS2 expression²², although this phenotype was not explored. In an unbiased approach, we analyzed the secretome of SPCS1^{-/-} 293T cells by mass spectrometry. Of the ~245 secreted proteins identified, only 35 were down-regulated in SPCS1^{-/-} cells, and fold-changes were small (Extended Data Figure 10 and Supplementary Table 4). We validated 3 of 5 as reduced in supernatants of SPCS1^{-/-} cells (Supplementary Table 5). Despite profound effects on flavivirus protein processing, an absence of SPCS1 modestly impacted expression of host proteins.

The differential requirement of SPCS1 for viral and host protein processing suggests that components of the SPCS complex in mammalian and likely insect cells facilitate cleavage of particular signal peptides in specific contexts. There may be additional requirements for some viruses as interactions between SPCS1 and the HCV NS2 and E2 proteins have been reported²³.

A recent study performed an analogous CRISPR-based screen with WNV²⁴. ER-associated genes were identified that prevented WNV-induced cell death. We identified three of these genes (*EMC4*, *EMC6*, and *SEL1L*), as did an siRNA screen²⁵. Virtually all human gene ‘hits’ identified in our screen had insect orthologs required for optimal flavivirus infection. A subset of our genes also were identified in RNAi screens in *Drosophila* cells^{26,27}. The ER is a focal site in the flavivirus lifecycle because it supports translation, polyprotein processing, replication, and virion morphogenesis. The identification of host gene targets selectively required for flavivirus infection but not cell survival provide intriguing candidates for pharmacological inhibition.

METHODS

Cells and viruses

Vero, BHK21, HeLa, U2OS, Huh7.5, and 293T cells were cultured at 37°C in Dulbecco’s Modified Eagle Medium supplemented with 10% fetal bovine serum (FBS). C6/36 *Aedes albopictus* cells were cultured at 28°C in L15 supplemented with 10% FBS and 25 mM HEPES pH 7.3. *Drosophila* DL1 cells were cultured at 28°C in Schneiders’ medium supplemented with 10% FBS as described²⁸. Jurkat cells were cultured at 37°C in RPMI 1640 supplemented with 10% FBS and 10 mM HEPES pH 7.3. All cell lines were tested and judged free of mycoplasma contamination. The following viruses were used in screening and validation studies: WNV (New York 2000), WNV (Kunjin), JEV (14-14-2 vaccine and Bennett strains), DENV-2 (16681 and New Guinea C strains), ZIKV (H/PF/2013), YFV (17D vaccine), CHIKV (2006 La Reunion OPY1), LACV (original strain), VSV (Indiana), HCV (J6/JFH), and SINV (Toto). With the exception of HCV (see below), all other viruses were propagated in BHK21, Vero, or C6/36 cells and titrated by standard plaque or focus-forming assays²⁹.

Viral growth analysis

293T or Huh7.5 cells were infected with WNV (MOI of 0.01), JEV (14-14-2 strain, MOI of 0.05 or 0.5; Bennett strain, MOI of 0.05), DENV-2 (MOI of 3), YFV (MOI of 1), ZIKV (MOI of 0.05), CHIKV (MOI of 0.01), SINV (MOI of 0.01), RVFV (MOI of 1), or VSV (MOI of 0.01). After 2 h of incubation, cells were washed three times and samples were titrated on Vero cells. For HCV growth analysis, control and SPCS1 gene-edited Huh7.5 cells were inoculated at an MOI of 1 with virus derived from a growth adapted JFH-1 infectious clone³⁰. Cells were rinsed six hours after infection to remove unbound virus and samples were collected every 24 hours for 7 days. Viral titers in the supernatant were quantified by focus-forming assay as described previously³¹.

Pooled sgRNA screen and data analysis

A pooled library encompassing 122,411 different sgRNA against 19,050 human genes was derived by the Zhang laboratory³² and obtained from a commercial source (Addgene). The library was packaged using a lentivirus expression system and 293T cells were transfected using Fugene®HD (Promega). Forty-eight hours after transfection, supernatants were harvested, clarified by centrifugation (3,500 RPM × 20 min), filtered, and aliquotted for storage at -80°C.

For the screen, we generated clonal 293T-Cas9 cells by transfecting the lentiCas9-Blast plasmid (Addgene #52962) using Fugene®HD transfection reagent (Promega), blasticidin selection, and limiting dilution. These 293T-Cas9 cells were transduced with lentiviruses encoding individual sgRNA at a multiplicity of infection (MOI) of 0.3. After selection with puromycin for 7 days, $\sim 2 \times 10^8$ cells were infected with WNV (MOI of 1) and then incubated for 2 to 3 weeks. In parallel, untransduced 293T-Cas9 cells were infected to ensure virus-induced infection and cell death. The experiments were performed in parallel as either duplicate or triplicate technical replicates in two independent biological experiments.

Genomic DNA was extracted from the uninfected cells (5×10^7) or the cells (3×10^7) that survived WNV infection, and sgRNA sequences were amplified⁵, and subjected to next generation sequencing using an Illumina HiSeq 2500 platform, and the sgRNA sequences against specific genes were recovered after removal of the tag sequences using the FASTX-Toolkit (http://hannonlab.cshl.edu/fastx_toolkit/) and cutadapt 1.8.1.

Gene validation

The cut-off of for candidate gene ‘hits’ was made using a published computational tool (MAGeCK)⁸ and reflected sequencing data showing multiple different sgRNA per gene, the number of sequencing reads per gene, the enrichment of a given sgRNA compared to the uninfected cell library (see Supplementary Tables 1 and 2). From this, we identified 12 genes that showed statistically significant enrichment compared to uninfected cells. These candidate genes were tested for validation by using 3 to 5 independent sgRNA per gene from the parent library and cloning them into the plasmid pSpCas9(BB)-2A-Puro (PX459) V2.0 (Addgene plasmid 62988). The control sgRNAs were utilized from the parent library. Plasmids were transfected into 293T or HeLa cells using Fugene®HD transfection reagent

and puromycin was added one day later. Three days later, puromycin was removed, and cells were allowed to recover for three additional days prior to infection with different viruses.

For flow cytometric analyses, gene-edited 293T were infected with WNV (MOI of 5, 12 h), JEV (MOI of 50, 22 h), ZIKV (MOI of 10, 30 h), DENV-2 (MOI of 3, 32 h), YFV (MOI of 3, 38 h), CHIKV (MOI of 1, 6 h), SINV (MOI of 10, 6 h), LACV (MOI of 5, 6 h), or VSV-GFP (MOI of 1, 5.5 h). Gene-edited HeLa cells were infected with WNV (MOI of 3, 24 h). At the indicated times, cells were fixed with 1% paraformaldehyde (PFA) diluted in PBS for 20 min at room temperature and permeabilized with Perm buffer (HBSS (Invitrogen), 10 mM HEPES, 0.1% (w/v) saponin (Sigma), and 0.025% NaN_3 (Sigma)) for 10 min at room temperature. Cells then were rinsed one additional time with Perm buffer, transferred to a U-bottom plate, and incubated for 1 h at 4°C with 1 $\mu\text{g}/\text{ml}$ of the following virus-specific antibodies: WNV (human E16³³); DENV2 (mouse E18³⁴); JEV (mouse E18³⁴); YFV (mouse E60³⁴); CHIKV (CHK-11³⁵); SINV (ascites fluid, ATCC VR-1248AF), LACV (807-31 and 807-33, gift of A. Pekosz, Baltimore, MD). After washing, cells were incubated with an Alexa Fluor 647-conjugated goat anti-mouse or anti-human IgG (Invitrogen) for 1 h at 4°C. Cells were fixed in 1% PFA in PBS, processed on a FACS Array (BD Biosciences), and analyzed using FlowJo software (Tree Star).

Validation also was performed by an infectious virus yield assay. Bulk gene-edited 293T cells were infected with WNV (MOI, 0.01) or JEV (MOI, 0.5). Supernatants were harvested at specific times after infection and focus-forming assays were performed in 96-well plates as described previously³⁶. Following infection, cell monolayers were overlaid with 100 μl per well of medium (1 \times DMEM, 4% FBS) containing 1% carboxymethylcellulose, and incubated for 22 (WNV) or 36 (JEV) h at 37°C with 5% CO_2 . Cells were then fixed by adding 100 μl per well of 1% PFA directly onto the overlay at room temperature for 40 minutes. Cells were washed twice with PBS, permeabilized (in 1 \times PBS, 0.1% saponin, and 0.1% BSA) for 20 minutes, and incubated with cross-reactive antibodies specific for WNV (humanized E16³³) or JEV (mouse E18³⁴) E glycoprotein for 1 h at room temperature. After rinsing cells twice, cells were incubated with species-specific HRP-conjugated secondary antibodies (Sigma). After further washing, foci were developed by incubating in 50 $\mu\text{l}/\text{well}$ of TrueBlue peroxidase substrate (KPL) for 10 min at room temperature, after which time cells were washed twice in water. Well images were captured using Immuno Capture software (Cell Technology Ltd.), and foci counted using BioSpot software (Cell Technology Ltd.).

Insect cell and fly infections

dsRNAs were generated as described³⁷. To silence genes using RNAi, insect cells were passaged into serum-free media containing dsRNAs targeting the indicated genes. Cells were serum-starved for one hour, after which complete media was added and cells were incubated for 3 days. Cells were infected with WNV (Kunjin strain) at an MOI of 4 or DENV-2 (NGC strain) at an MOI of 1 for 30 h and then processed for microscopy with automated image analysis as described³⁸. Control (*hs>+*) or dSPCS3-depleted (*hs>dSPASE22-23* (SPCS3) IR (Bloomington)) 4 to 7 day-old female flies were heat shocked (37°C) for 1 h for three consecutive days to deplete the gene of interest and

challenged with WNV (Kunjin) (5 PFU). At day 7 after infection, pools of 10 flies were crushed and titered by plaque assay. Three independent experiments were performed. Heterozygous flies (Spase12(EY10774)) were outcrossed to wild-type flies and either wild-type or Spase12 heterozygous sibling controls were challenged with Kunjin for 7 days and groups of 5 flies were titered.

siRNA treatments in human cells

Human U2OS cells were transfected with siRNAs against control, SPCS1, SPCS2, or SPCS3 genes for three days, infected with WNV (Kunjin strain) or DENV (MOI, 1) for 18 h, and then processed for microscopy with automated image analysis as described³⁸.

Replicon transfection and analysis

Two types of replicons were used. **(a) SP6-generated YFV replicons.** The WT and NS5 polymerase mutant (GDD→GVD) YFV replicons (YF-FFLuc2A, WT and GVD) have been published previously¹² and were the generous gift of R. Kuhn (West Lafayette, IN). Capped replicon RNA was generated using SP6 polymerase with a mMACHINE kit according to the manufacturer's instructions (Thermo Fisher Scientific). RNA was purified using an RNEasy kit (Qiagen) and 2 µg was transfected into control or SPCS1^{-/-} Huh7.5 cells using Lipofectamine 3000 according to the manufacturer's instructions (Thermo Fisher Scientific). At specified times, cells were harvested, lysed, and processed for firefly luciferase activity using a commercial kit (Promega). Cleared lysates were tested for Fluc activity using the Dual-Luciferase Reporter Assay System (Promega) and the protein concentration was quantified using a BCA assay kit (ThermoFisher). Fluc activity (relative light units, RLU) was normalized by subtracting background luminescence of transfected cells collected at the time of transfection, then the adjusted RLU was divided by the total protein content (in µg) to yield RLU per µg protein. **(b) cDNA launched WNV replicons.** The construction of WT and NS5 polymerase mutant (GDD→GVD) WNV replicons (lineage I, strain New York 1999) was based on a previously described cDNA launched molecular clone system³⁹. The backbone of this strategy, a plasmid containing a truncated WNV genome under the control of a CMV promoter (pWNV-backbone), was designed to be complemented via ligation of a structural gene DNA fragment; transfection of pWNV-backbone alone does not result in production of a self-replicating RNA molecule. Using overlap extension PCR and unique restriction endonuclease sites, pWNV-backbone was modified by the introduction of a fragment downstream of the CMV promoter encoding [5'UTR-cyclization sequence of capsid-FMDV2a protease-signal sequence of E-NS1] to complement the NS2→NS5-3'UTR already present in the pWNV-backbone plasmid, generating the replicon plasmid pWNVI-rep. The reporter gene GFP then was cloned upstream of the FMDV2a protease sequence via a unique MluI site to generate pWNVI-rep-GFP. The construction and organization of this WNV lineage I replicon is analogous to a previously described lineage II WNV replicon (pWNVIIrep-GFP)⁴⁰. Finally, QuikChange mutagenesis (Agilent Technologies) was used to delete the enhancer portion of the CMV immediate early enhancer/promoter, generating pWNVI-minCMV-rep-GFP, and to generate the GDD→GVD NS5 polymerase variant. Although the CMV enhancer/promoter combination commonly found in cloning vectors results in robust and constitutive expression, inclusion of only the minimal CMV promoter (no enhancer) results in low level

expression⁴¹. As such, direct transfection of pWNVI-minCMV-rep-GFP results in a dim GFP signal, which reflects translation of the RNA generated by DNA-dependent RNA translation. RNA polymerase-dependent replication of the WT (but not GVD mutant) replicon results in higher production of GFP over time. The eGFP is bracketed by the FMDV2a autocleavage site, and does not rely on host or viral proteases for processing. WT and NS5 GVD variants of pWNVI-minCMV-rep-GFP (200 ng) were transfected into 10⁴ control or gene-edited 293T cells (96 well plates) using Lipofectamine 2000. At various times after transfection, cells were harvested, cooled to 4°C, stained sequentially with a biotinylated anti-9NS1⁴² (or biotin anti-CHIKV negative control MAb) and Alexa 647 conjugated streptavidin. In some samples, cells were fixed with 4% PFA in PBS (10 min, room temperature) and permeabilized with 0.1% saponin (w/v). Cells were processed for two-color flow cytometry using a MACs Quant Analyzer 10 (Miltenyi Biotec).

Plasmid transfections

293T gene edited cells were transfected with the following genes that were derived from a WNV infectious cDNA clone⁴³ and then cloned into a pHLsec backbone (gift of D. Fremont, St Louis, MO): V5-C-prM-E, prM, prM-FLAG (3X FLAG), E, prM-E, prM-E-NS1, E-NS1, NS1, NS1-NS2A-FLAG (includes full-length NS1 and 231 amino acids of NS2A fused to a C-terminal 3X FLAG), and 2K-NS4B-hemagglutinin tag (HA). These plasmids were obtained from colleagues (2K-NS4B-HA⁴⁴, gift of A. Garcia-Sastre, New York) or in some cases engineered to contain either native WNV signal sequences (C-prM, 18 amino acids beyond the C-terminus of C; prM-E, 17 C-terminal amino acids of prM; E-NS1, 24 C-terminal amino acids of E) or the signal sequence of mouse K^b class I MHC (N-terminal 21 amino acids). Plasmids were transfected into gene-edited 293T cells using Fugene®HD reagent (Promega) according to the manufacturer's instructions. Supernatants containing prM-E subviral particles (SVPs) were collected 24 h after transfection, filtered through a 0.2-µm filter, and stored aliquotted at -80°C. For the capture ELISA, Nunc MaxiSorp polystyrene 96-well plates were coated overnight at 4°C with mouse E60 mAb³⁴ (5 µg/ml) in a pH 9.3 carbonate buffer. Plates were washed three times in enzyme-linked immunosorbent assay (ELISA) wash buffer (PBS with 0.02% Tween 20) and blocked for 1 h at 37°C with ELISA block buffer (PBS, 2% bovine serum albumin, and 0.02% Tween 20). Supernatants from prM-E plasmid transfected cells were captured on plates coated with E60 for 90 min at room temperature (RT). Subsequently, plates were rinsed five times in wash buffer and then incubated with humanized anti-WNV E16 (1 µg/ml in block buffer) in triplicate for 1 h at RT. Plates were washed five times and then incubated with pre-absorbed biotinylated goat anti-human IgG antibody (1 µg/ml; Jackson Laboratories) for 1 h at RT in blocking buffer. Plates were washed again five times and then sequentially incubated with 2 µg/ml of horseradish peroxidase-conjugated streptavidin (Vector Laboratories) and tetramethylbenzidine substrate (Dako). The reaction was stopped with the addition of 2 N H₂SO₄ to the medium, and emission (450 nm) was read using an iMark microplate reader (Bio-Rad).

Western blotting

For virus infected samples, cells were infected with WNV (MOI of 200 to 1000, 24 h), JEV (MOI of 150, 45 h), CHIKV (MOI of 5, 12 h), SINV (MOI of 5, 16 h), RVFV (MOI of 2.5,

16 h), or HCV (MOI of 5, 48 or 72 h). Cells (10^6) were lysed directly in 30 μ l RIPA buffer (Cell Signaling) with 0.1% SDS and a cocktail of protease inhibitors (Sigma-Aldrich). Samples were prepared in LDS buffer (Life Technologies) under non-reducing or reducing (dithiothreitol) conditions. After heating (70°C, 10 min), samples were electrophoresed using 7% Tris-Acetate or 4–12%, 10% or 12% Bis-Tris gels (Life Technologies) and proteins were transferred to PVDF membranes using an iBlot2 Dry Blotting System (Life Technologies). Membranes were blocked with 5% non-fat dry powdered milk and probed with antibodies against SPCS1 (11847-1-AP, Proteintech), SPCS2 (14872-1-AP, Proteintech), SPCS3 (ab91222, Abcam), SEC11A (14753-1-AP, Proteintech), SEC11C (HPA026816, Sigma) and SEC61B (ab15576, Abcam). For studies with prM-E, prM, E, NS1, NS1-2A-FLAG, or 2K-NS4B-FLAG transfected or virus-infected cells, membranes were probed with anti-E (human E16; mouse CHK-48³⁵; mouse anti-JEV, oligoclonal pool), anti-NS1 (mouse 8-NS1), anti-NS3 (W1018-54, USBio), anti-NS4B (rabbit polyclonal antibody⁴⁵, gift of W.I. Lipkin, New York, NY) anti-prM (human CR4293¹⁶ or rabbit WNV-M (IMG-5099A, IMGEX)), anti-FLAG (F1804, Sigma), and the relevant secondary antibodies. For validation of the secretome experiments, supernatants were electrophoresed and PVDF membranes were probed with anti-CXCL16 (ab101404, Abcam), anti-SFRP1 (ab126613, Abcam), anti-RNASET2 (ab169655, Abcam), anti-LGALS3BP (ab81489, Abcam), anti-SLITL2 (ab173758, Abcam), anti-PEDF (ab157207, Abcam), anti-NPC2 (19888-1-AP, Proteintech), anti-CREG1 (12220-1-AP, Proteintech), and the relevant secondary antibodies. Western blots were developed using SuperSignalTM West Pico Chemiluminescent Substrate or SuperSignalTM West Femto Maximum Sensitivity Substrate (Life Technologies).

Metabolic labeling, pulse-chase, and immunoprecipitation experiments

Pulse- and pulse-chase experiments were performed as described previously⁴⁶. After starvation in methionine/cysteine-free DMEM for 30 min, 293T cells were labeled metabolically with 300 or 500 μ Ci/ml of [³⁵S]-methionine/cysteine (PerkinElmer Life Sciences) at 37°C for 3 or 40 min. Cells then were washed three times in PBS and immediately lysed or incubated in DMEM supplemented with non-radiolabeled cysteine (500 μ g/ml) and methionine (100 μ g/ml). Cells lysis was performed in 400 μ l of 50 mM Tris-HCl, pH 7.4, 150 mM NaCl, 1 mM PMSF, 1 mM EDTA, 5 μ g/ml aprotinin, 5 μ g/ml leupeptin, 1% Triton X-100, 1% sodium deoxycholate, 0.1% SDS. After preclearing with an irrelevant human MAbs protein A-agarose (Thermo Fisher Scientific) complex, lysates were incubated for 1 h at 4°C with humanized monoclonal E16 and E60 MAbs or anti-FLAG and then with protein A-agarose for 2 h. The immunoprecipitates were washed seven times in 50 mM Tris-HCl, pH 7.4, 150 mM NaCl, 1 mM PMSF, 1 mM EDTA, 5 μ g/ml aprotinin, 5 μ g/ml leupeptin, 1% Triton X-100, 1% sodium deoxycholate, and 0.1% SDS, and then analyzed by SDS-PAGE under reducing conditions, followed by fluorography. Some immunoprecipitates were incubated with 20 milliunits of endoglycosidase H or PNGase F (New England BioLabs) for 1 h at 37°C prior to SDS-PAGE and fluorography.

293T cell viability assay

A Vybrant MTT cell viability assay (Life Technologies) was used according to the manufacturer's instructions. Briefly, 10 μ l of 12 mM MTT (4,5-dimethylthiazol-2-yl-2-5-

diphenyltetrazolium bromide) was added to 10^5 293T cells (different gene-edited lines, with or without WNV infection) in 100 μ l of phenol-red free medium. Cells were incubated for 4 h at 37°C, at which time medium was removed and formazan crystals solubilized in 100 μ l of DMSO were added for 10 min at 37°C. Liquid was analyzed for absorbance at 540 nm using a Synergy H1 Hybrid Plate Reader (Biotek).

Flow and mass cytometry analysis of Jurkat T cells

The antibodies and conjugates used are listed in Supplemental Table 6. For flow cytometry studies, WT and SPCS1 gene-edited Jurkat T cells were incubated with fluorophore-conjugated MAbs for 30 min at 4°C and then washed three times in PBS containing 5% FBS. Cells were immediately processed on an LSRII flow cytometer and data were analyzed using FlowJo 10.0.7. For mass cytometry studies, WT and SPCS1 gene-edited Jurkat T cells were labeled with MAbs conjugated with transition element isotopes and analyzed on a CyTOF 2 mass cytometer (Fluidigm DVS Sciences). Data were analyzed using Cytobank (<http://wustl.cytobank.org>) and FlowJo 10.0.7.

Secretome analysis of SPCS1^{-/-} 293T cells

WT and SPCS1^{-/-} 293T cells were cultured in poly-D-lysine treated flasks in FreeStyle™ 293 Expression Medium (ThermoFisher) supplemented with 10% FBS. At 90% confluence, cells were washed four times with pre-warmed PBS, then two times with pre-warmed FreeStyle™ 293 Expression Medium, and maintained in FreeStyle™ 293 Expression Medium without FBS for 48 h. Supernatants were harvested and clarified by centrifugation at 1,000 g for 5 min, and then 10,000 g for 20 min at 4°C. Samples were concentrated with Amicon Ultra-15 Centrifugal Filter Units (Millipore) at 5,000 g for 1 h in the presence of 1 \times protease inhibitors (Catalog # S8830, Sigma). The concentrates were collected and stored at -80°C. After thawing on ice, the samples were exchanged twice in digestion buffer (Tris, 0.1 M, pH 8.5 containing 8 M urea) by centrifugation (~4,000 \times g, 2 h) in Amicon Ultracel 3K units to a volume of ~100 μ l. The solubilized samples were reduced with 2 mM DTT (ThermoScientific) for 30 min at 37°C followed by alkylation at room temperature for 30 min with 7 mM iodoacetamide (Sigma) in the dark. The alkylated samples were treated with 7 mM DTT for 15 min at room temperature. After dilution, the samples were digested with LysC (1 μ g) (Sigma) overnight at 37°C with agitation (ThermoMixer). After dilution of the samples to 1.5 M urea with Tris buffer, trypsin was added (5 μ g) (Sigma) was added and the incubation was continued overnight at 37°C with mixing. The digested samples were acidified with to a concentration of 1% tri-flouro acetic acid (TFA). The peptides were desalted with a SepPak (50 mg) with 0.1% TFA/70% acetonitrile in an elution volume (2 ml). The lyophilized peptides were quantified with a fluorescent assay (Thermo Fisher) and 2 μ g was labeled with TMT-6 reagents according to the vendor. The labeled peptides were desalted and the samples were transferred to PCR tubes (0.5 ml) and positioned in 96-well holders for robotic solid phase extraction (SPE). Each digest was extracted sequentially with one C4 tip (Glygen BIOMEK NT3C04) and one porous graphite carbon micro-tip (Glygen BIOMEK NT3CAR) with the following auto-pipetting steps: (i) wet tips with AcN/FA (60%/1%) (10 \times 25 μ l); (ii) equilibrate tips with AcN/FA (1%/1%) (10 \times 25 μ l); (iii) extract peptides with repetitive aspirations of the digest (50 \times 25 μ l); (iv) wash loaded tips with AcN /FA (1%/1%) (10 \times 25 μ l); and (v) elute peptides with AcN/FA (60%/1%) (5 \times 65 μ l).

The SPE eluents were pooled and dried in a SpeedVac centrifuge and transferred to an autosampler vial for LC-MS analysis.

The remainder of the peptides were dissolved in the binding buffer (100 mM Tris, pH 7.8 containing NaCl (0.5 M), MnCl₂ (1 mM) and CaCl₂ (1 mM). The dried lectins (Con-A and WGA) Sigma were dissolved in binding buffer (4 mg/mL). The rCA120 (10 mg/ml), Con-A and WGA were added to the peptide solution (36 µl and 10 µl, respectively). After incubation at room temperature, the mixture was transferred to a YM-10 Microcon filter unit. After centrifugation (14,000 × g) for 10 min and washing with binding buffer (100 µl), the filter unit was transferred to another tube. The peptides were released with the addition of PNGase (10 units) in 100 µl of ammonium bicarbonate buffer (50 mM) after incubation at 37C for 1.5 hours. The enzyme addition and incubation was repeated and the peptides recovered with one wash of PNGase buffer. The peptides were acidified to 5% formic acid and desalted, labeled with TMT-6, and prepared for LC-MS as described above for the total pool of peptides.

LC/MS Analysis

LC-ESI/MS/MS analysis was conducted with a Q-Exactive Plus mass spectrometer coupled to an EASY-nanoLC 1000 system (Thermo-Fisher). For each Hp-RP fraction, 2 µl of sample was loaded onto a 75 µm i.d. × 25 cm Acclaim[®] PepMap 100 RP column (Thermo-Fisher Scientific). Peptide separations were started with 95% mobile phase A (0.1% FA) for 5 min and increased to 30% B (100% ACN, 0.1% FA) over 180 min, followed by a 25 min gradient to 45% B, a 5 min gradient to 95% B and wash at 90% B for 7 min, with a flow rate of 300 nl/min. Full-scan mass spectra were acquired by the Orbitrap mass analyzer in the mass-to-charge ratio (*m/z*) of 375 to 1400 and with a mass resolving power set to 70,000. Fifteen data-dependent high-energy collisional dissociations were performed with a mass resolving power set to 35,000, a fixed first *m/z* 100, an isolation width of 0.7 *m/z*, and the normalized collision energy (NCE) setting of 32. The maximum injection time was 50 ms for parent-ion analysis and 105 ms for product-ion analysis. Target ions already selected for MS/MS were excluded dynamically for 30 sec. An automatic gain control target value of 3e6 ions was used for full MS scans and 1e5 ions for MS/MS scans. Peptide ions with charge states of one or greater than six were excluded from MS/MS interrogation.

Protein Identification and Quantification with TMT

All raw data were processed using Proteome Discoverer (version 2.1.0.81, Thermo-Fisher Scientific). MS/MS spectra were searched with SequestHT engine against the human UniRef database (69,021 entries; version 2014_05), assuming the digestion enzyme was trypsin with a maximum of 2 missed cleavage allowed. The searches were performed with a fragment ion mass tolerance of 0.02 Da and a parent ion tolerance of 20 ppm. Deamidation of asparagine and glutamine, acetylation and TMT 6-plex derivatization of N-terminus and oxidation of methionine were specified in Proteome Discoverer as variable modifications. Iodoacetamide derivatization of cysteine and TMT 6-plex derivatization of lysine were specified as fixed modifications. Peptide spectral matches (PSM) were validated using percolator based on *q*-values at a 1% FDR⁴⁷. Peptides were filtered to 1% FDR and grouped into proteins at 1% FDR as specified in Proteome Discoverer. The intensities of TMT reporter ions were

determined with Proteome Discoverer at a mass tolerance of 0.01 Da and used for peptide quantifications. The median values of peptide intensities that can be assigned to a same protein was used to represent protein intensities. Peptide identifications that can be assigned to more than one protein were removed from protein quantification

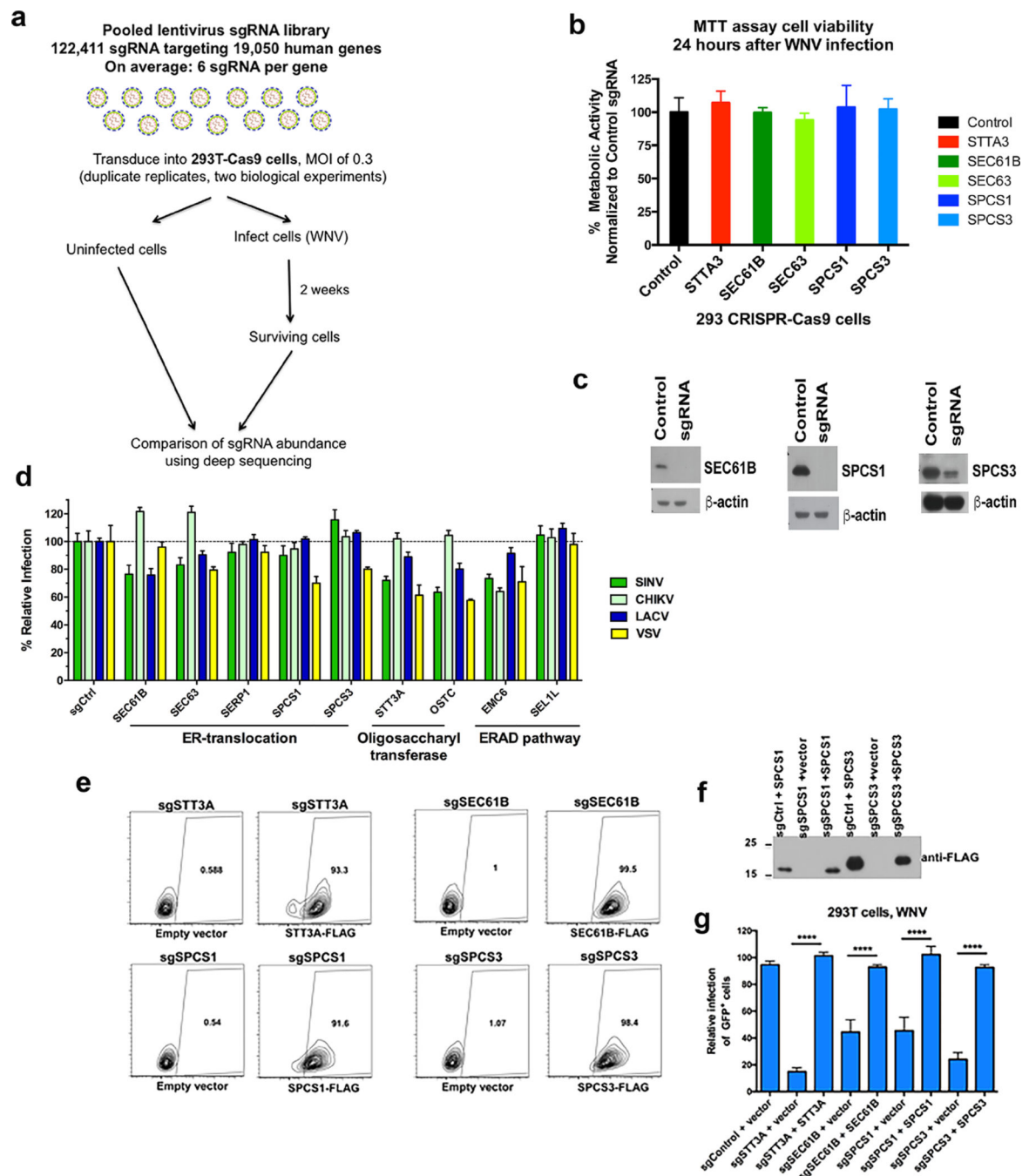
Proteomic Data Analysis

Normalization in protein ratios was applied in that the median ratios are log₂ zero. Data analysis was performed with the free software environment for statistical computing and graphics, R (<http://www.R-project.org>). Gene ontology (GO) analysis was carried out using the Database for Annotation, Visualization and Integrated Discovery (DAVID)^{48,49}. Data from duplicated LC/MS/MS analysis were first averaged and protein abundance ratios were log₂ transformed prior to statistical analysis. A one-way ANOVA with Benjamini-Hochberg (BH) correction was performed to assess the statistical significance in protein abundance changes between wild type and SPCS1^{-/-} cells.

Statistical analysis

Statistical significance was assigned when *P* values were < 0.05 using GraphPad Prism Version 5.04 (La Jolla, CA). Viral antigen staining after expression of sgRNA was analyzed using a one-way ANOVA adjusting for repeated measures with a Dunnett's multiple comparison test or with a Mann-Whitney test depending on the number of comparison groups. Analysis of levels of E protein in the supernatant from CRISPR-Cas9 gene edited cells was analyzed by a one-way ANOVA. Analysis of siRNA in insect and human cells was performed using a Student's T-test.

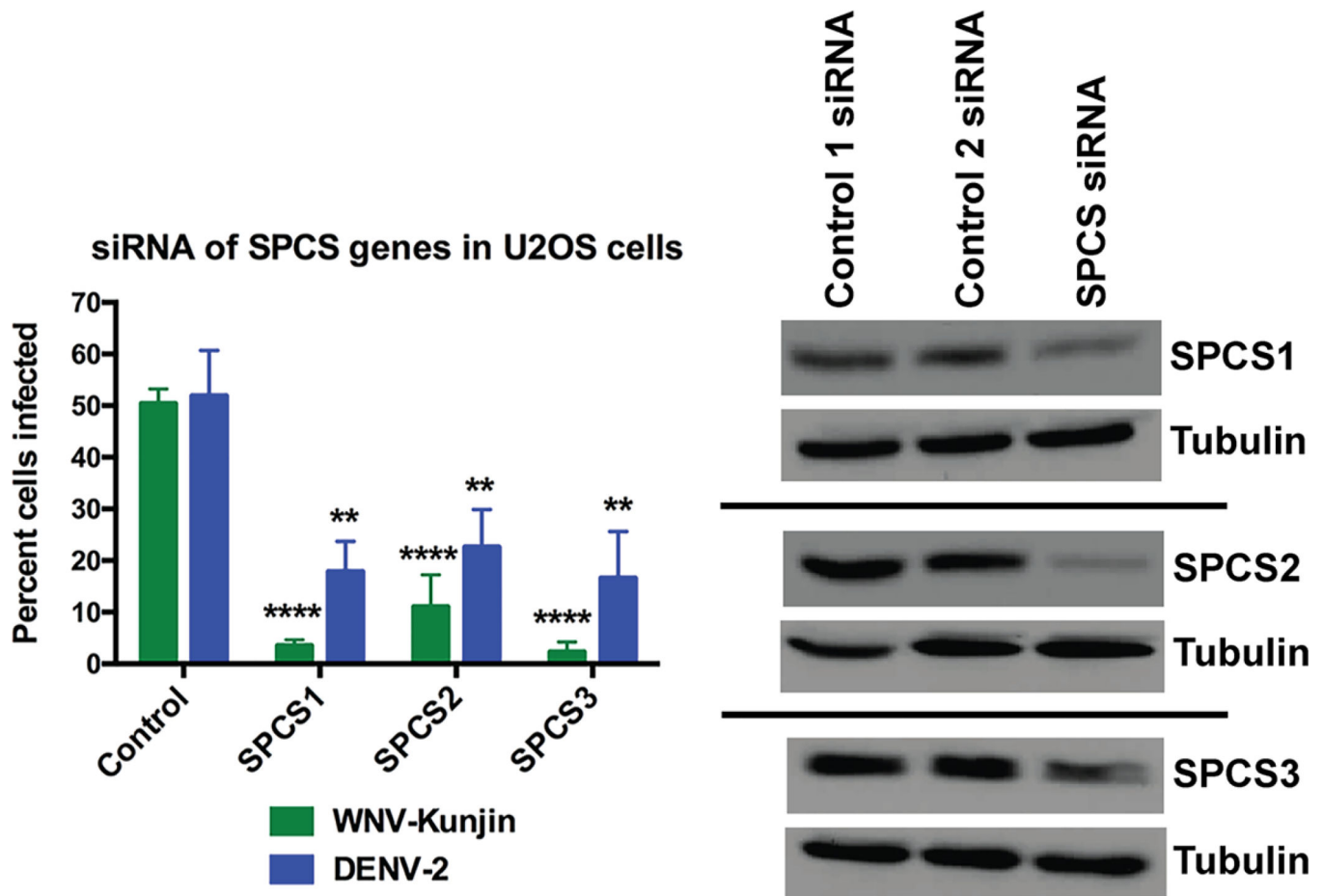
Extended Data



Extended Data Figure 1. Results of CRISPR-Cas9 screen

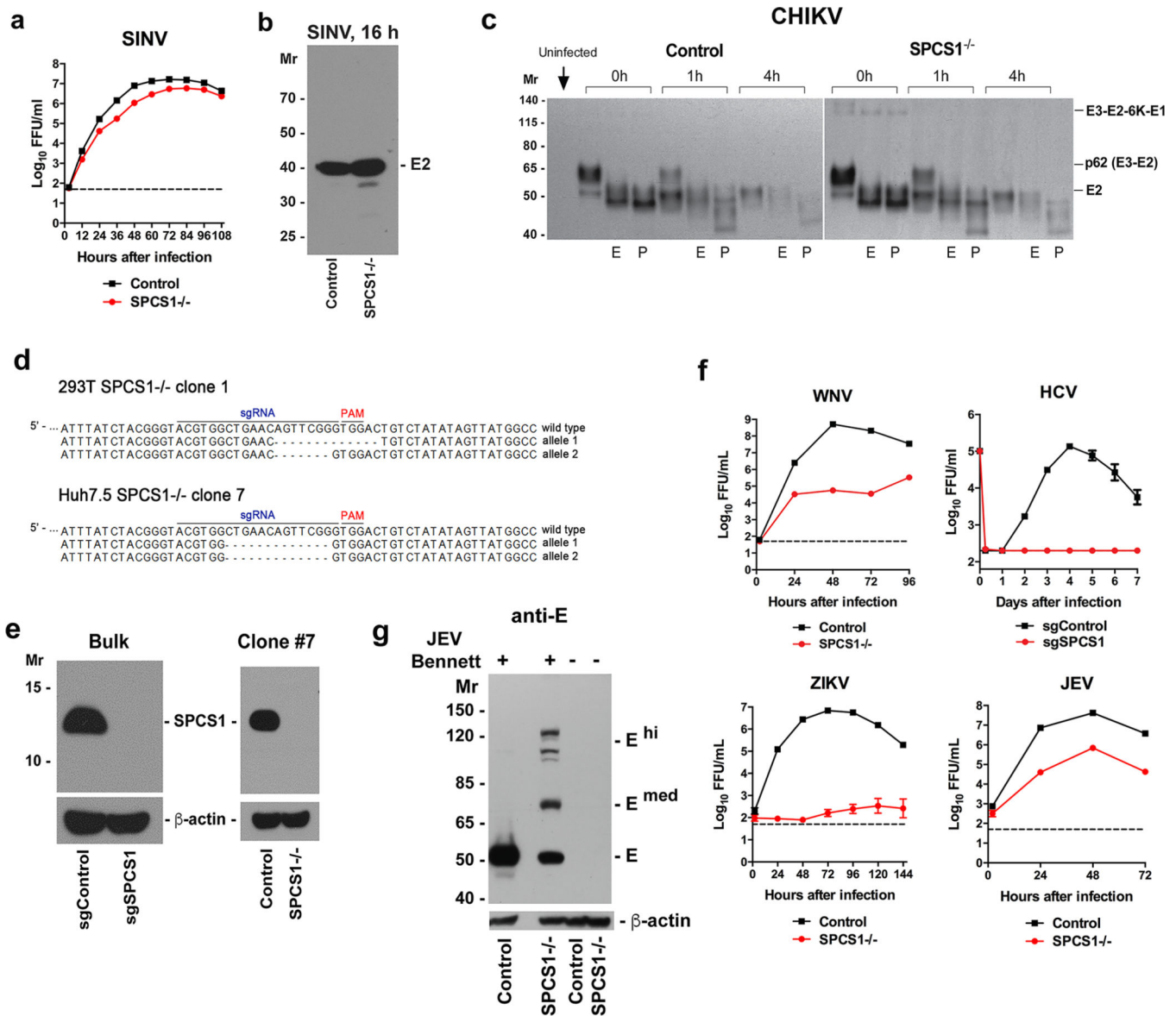
a. Scheme of gene-editing screen. **b.** Analysis of cell viability of gene-edited cells. WNV-infected CRISPR-Cas9 edited bulk cells were evaluated for cell viability using a metabolic MTT assay at 24 h post infection. The results were pooled from several independent experiments performed in duplicate and data were compared to cells edited with a control sgRNA. None of the differences were statistically different compared to the control. **c.** Western blotting confirms the efficiency of gene editing of *SEC61B*, *SPCS1*, and *SPCS3*. β -

actin is included as a loading control. **d.** Effect of gene editing on infection by other RNA viruses. sgRNA-edited bulk selected cell populations were infected with alphaviruses (SINV or CHIKV), a bunyavirus (LACV) or a rhabdovirus (VSV). Cells were analyzed for intracellular viral antigen staining by flow cytometry using virus-specific MAbs. The data is representative of two independent experiments and is expressed as relative infection (viral antigen expression) compared to the sgRNA control. **d–f.** Trans-complementation of sgRNA gene-edited cells with FLAG-tagged genes. **d.** Individual sgRNA bulk gene-edited cell lines were trans-complemented with cDNA expressing C-terminal FLAG-tagged versions of their respective genes and GFP or an empty vector control and GFP. Transfected cells were analyzed by flow cytometry for expression of the FLAG-tag in the GFP⁺ cells. The data is representative of two independent experiments. **e.** Western blotting of SPCS1 and SPCS3 trans-complemented genes after incubation with an anti-FLAG tag antibody. **f.** Individual sgRNA cell lines were trans-complemented with cDNA expressing C-terminal FLAG-tagged versions of their respective genes and GFP or an empty vector control and GFP. Transfected cells were infected with WNV (MOI of 5), and 12 h later, cells were stained for intracellular E antigen, and processed by flow cytometry. The data is representative of three independent experiments performed in triplicate and reflects the percentage of WNV-infected cells in the fraction that expressed GFP. The indicated comparisons were statistically different (****, $P < 0.0001$), as determined by the Mann-Whitney test. For gel source data, see Supplementary Figure 1.



Extended Data Figure 2. Gene silencing of SPCS genes in human U2OS cells

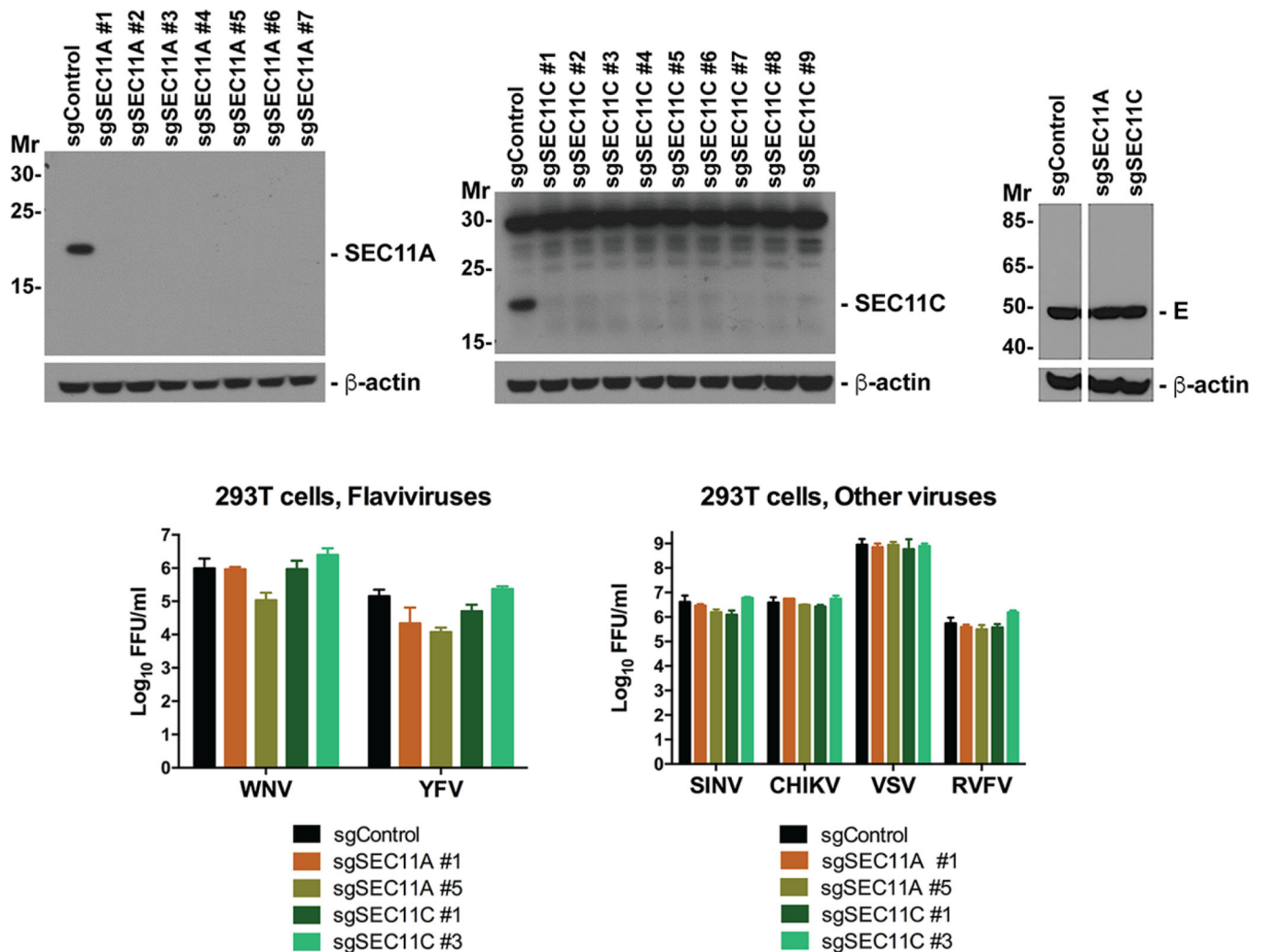
Human U2OS cells were transfected with either control or SPCS1, SPCS2, or SPCS3 siRNAs and infected with WNV (Kunjin strain) or DENV (MOI, 1) for 18 h. (*Left*) The percentage of infected cells was determined by automated fluorescence microscopy. The data is expressed as the mean normalized value \pm SD. Statistically significant differences (**, $P < 0.01$; ****, $P < 0.0001$ compared to control siRNA by ANOVA with a multiple comparison correction) are indicated. The data is pooled from three independent experiments assayed in quadruplicate. No reduction in infection of CHIKV or SINV was observed after SPCS gene silencing was observed (data not shown). (*Right*) Western blotting of SPCS proteins in gene silenced U2OS cells. Representative results are shown and tubulin is included as a loading control. For gel source data, see Supplementary Figure 1.



Extended Data Figure 3. Viral infection in SPCS1^{-/-} cells

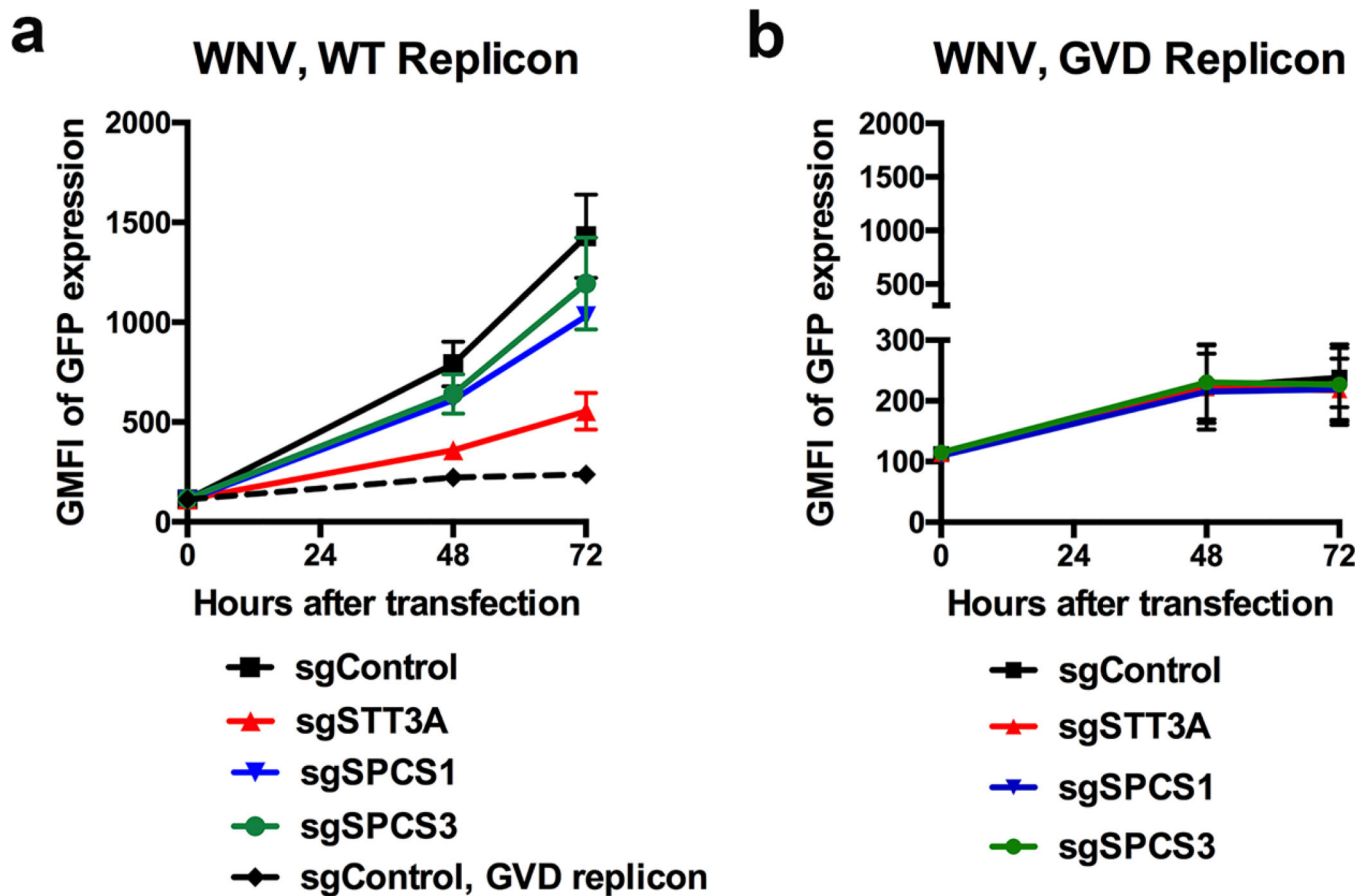
a–c. Alphaviruses replicate and are processed efficiently in 293T cells in the absence of expression of SPCS1. **a.** SINV infection in control and SPCS1^{-/-} clonal cells. Cells were infected (MOI of 0.01) and supernatants were harvested and analyzed by FFA. The results are the average of two independent experiments performed in triplicate. **b.** Control and SPCS1^{-/-} gene-edited 293T cells were infected with SINV. At the indicated time, lysates were prepared, electrophoresed and Western blotted with anti-SINV E2 ascites fluid (ATCC VR-1248AF). **c.** Control or SPCS1^{-/-} 293T cells were infected with CHIKV (MOI of 5). 8 h later, cells were labeled for 30 min with ³⁵S cysteine-methionine. Excess cold cysteine-methionine was added for indicated chase times (0, 1 or 4 h). An uninfected control established the specificity of the immunoprecipitation. After ³⁵S labeling, lysates were prepared and immunoprecipitated with anti-E2 MAbs (CHK-48). Immunoprecipitates were left untreated (blank) or treated with Endo H (E) or PNGase F (P) for 1 h at 37°C prior to

SDS-PAGE and fluorography. **d.** Sequencing of SPCS1 alleles in gene-edited 293T and Huh7 cell clones after puromycin selection and limiting dilution cloning. The sgRNA targeting site and the “PAM” sequences are highlighted at the top of WT gene, and the sequence of edited alleles are indicated. **e.** Western blotting of bulk-selected or clonal (clone #7) Huh7.5 cells (control and SPCS1 sgRNA selected) for expression of SPCS1 (~12 kDa). **f.** WNV, HCV, ZIKV, or JEV (Bennett strain) infection in control and SPCS1-deficient Huh7.5 cells. Cells were infected at an MOI of 0.01 (WNV, ZIKV, JEV) or 1 (HCV) and supernatants were harvested and analyzed by FFA. The results are the average of two independent experiments performed in triplicate. **g.** Control or SPCS1^{-/-} Huh7.5 cells were infected at an MOI of 150 for 45 h with a pathogenic JEV isolate (Bennett strain). Lysates were blotted with an anti-JEV E MAb. Higher molecular weight bands (E^{hi} and E^{med}) that reacted specifically with the anti-E MAb are indicated. One representative experiment of two is shown and loading controls (β -actin) are included. For gel source data, see Supplementary Figure 1.



Extended Data Figure 4. Gene editing of SEC11A and SEC11C do not substantially impact infection of several enveloped viruses

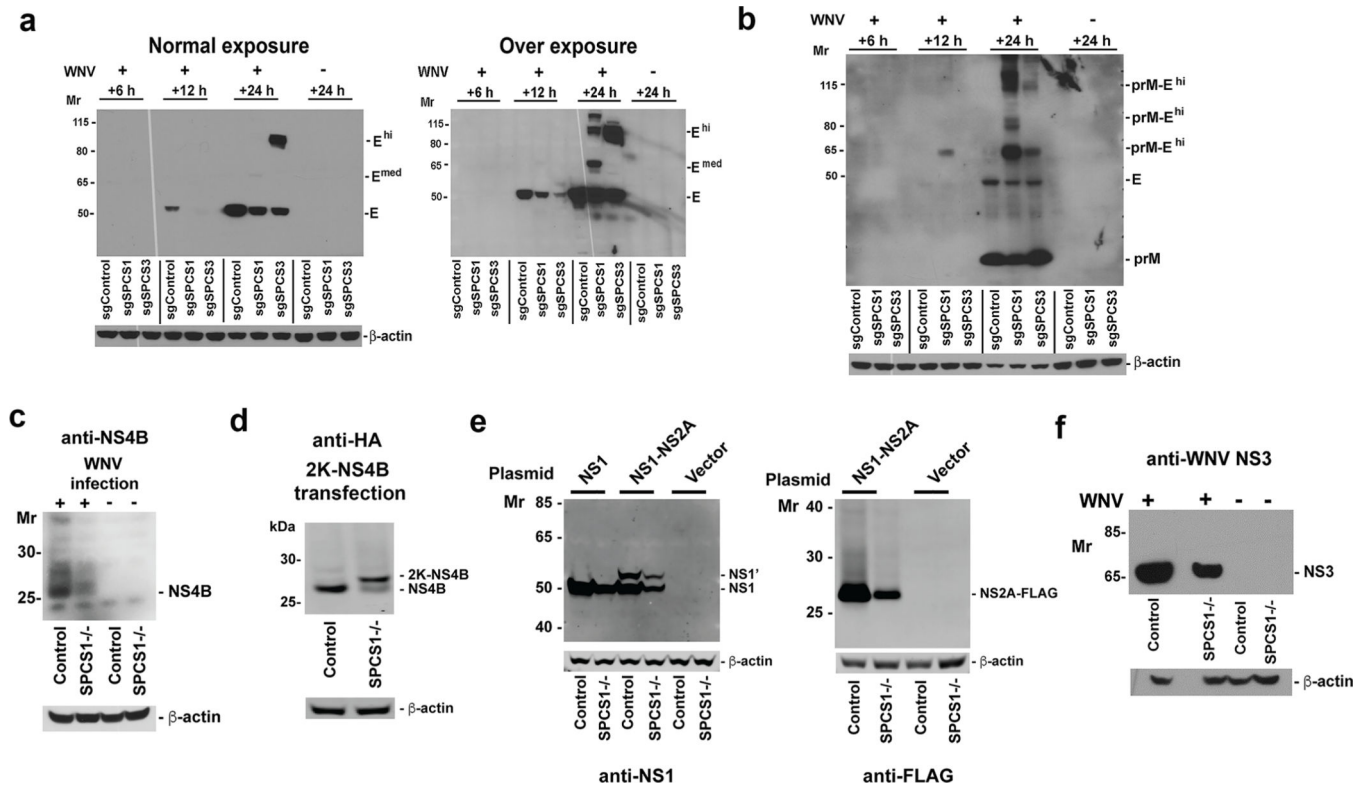
(*Top*) 293T cells were administered the indicated sgRNA and isolated in bulk after puromycin drug selection. Western blotting confirmed gene editing of SEC11A (*left*, 20 kDa) or SEC11C (*middle*, 22 kDa). No difference in levels or migration pattern of WNV E was observed in SEC11A or SEC11C gene edited cells (*right*) after WNV infection at an MOI of 200 for 24 h. Spaces between the Western blots indicate cropping to remove lanes that were not relevant to this experiment. (*Bottom*) Control or gene-edited 293T cells were infected with viruses and supernatants were harvested after infection for titration. *Left*, WNV (MOI of 0.01, 72 h) or YFV (MOI of 1, 72 h); *Right*, SINV (MOI of 0.01, 72 h), CHIKV (MOI of 0.01, 36 h), VSV (MOI of 0.01, 36 h), or RVFV (MOI of 1, 72 h). Results are representative of two independent experiments. For gel source data, see Supplementary Figure 1.



Extended Data Figure 5. Effect of sgRNA on translation and replication of a WT and NS5 GVD polymerase mutant WNV replicon

A cDNA launched WNV replicon (**a**, WT; **b**, GVD polymerase ‘dead’ mutant) with a minimal CMV promoter (GFP-NS1-NS2A-NS2B-NS3-NS4A-NS4B-NS5₃) was transfected into indicated gene-edited 293T cells. At 48 and 72 h after transfection, cells were harvested, and analyzed for GFP expression by flow cytometry. After transfection with the WT replicon, WNV replication was lower in STT3A gene-edited cells as determined by ANOVA with a multiple comparisons correction ($P < 0.05$ at 48 and 72 h). Data is the average of

three independent experiments. Note, the GVD replicon data with a sgRNA control (translation only) is provided for comparison in panel a.



Extended Data Figure 6. Processing of WNV proteins in SPCS1 and SPCS3 gene-edited 293T cells

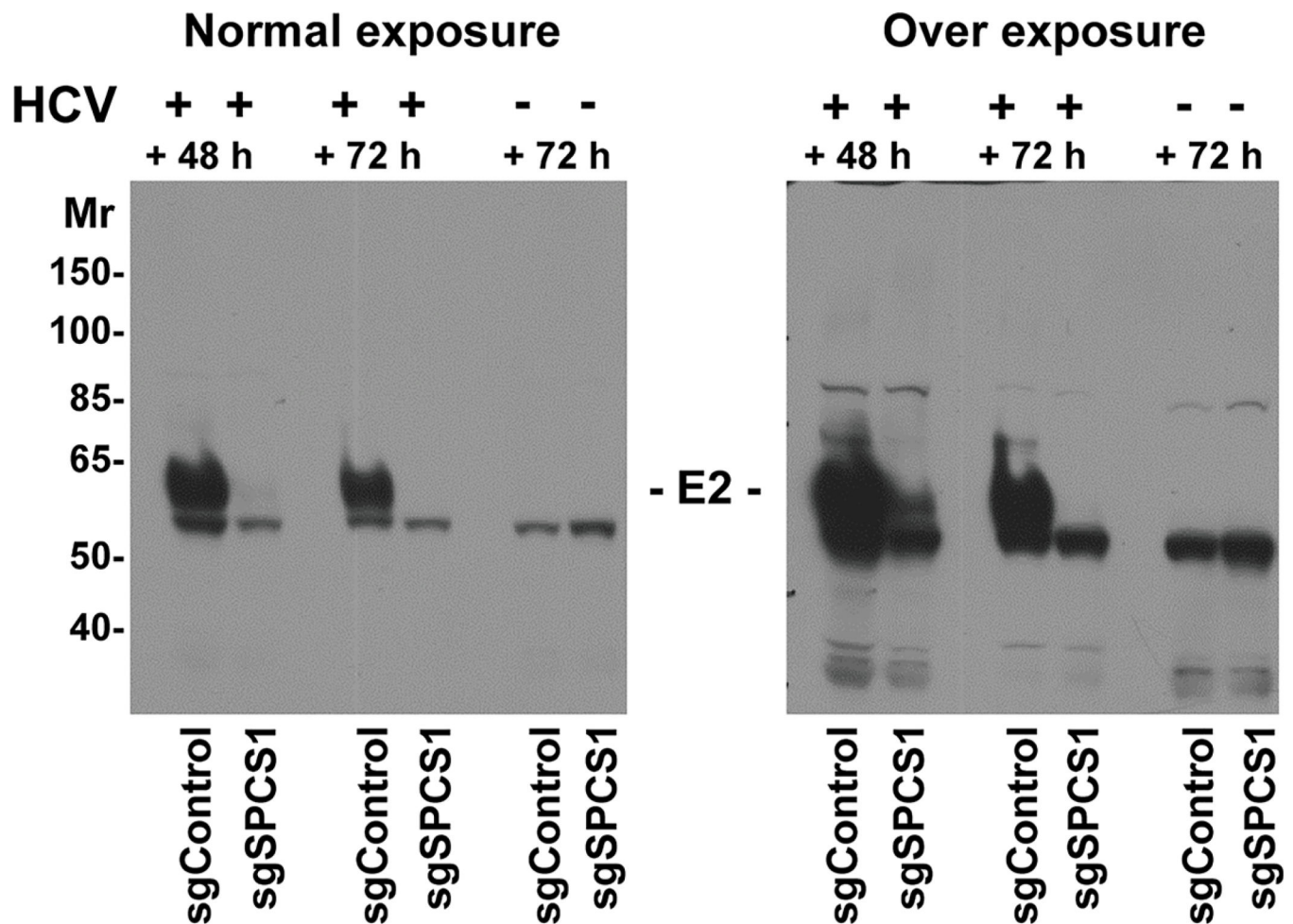
a. Normal (*left*) and over-exposed (*right*) Western blot in SPCS1 and SPCS3 bulk gene-edited 293T cells. The over-exposure is shown to highlight the accumulation of high molecular weight bands that react with anti-E protein antibody. Control, SPCS1, and SPCS3 gene-edited 293T cells were infected with WNV or mock-infected for the indicated times. Lysates were Western blotted with an anti-E (hE16) MAb. Under these electrophoresis conditions, natively processed E protein migrates at ~50 to 55 kDa. Higher molecular weight bands (E^{med} (likely prM-E) and E^{hi} (likely prM-E-NS1)) that react specifically with the E MAb are present only in SPCS1 and SPCS3 gene-edited 293T cells. The data is representative of two independent experiments and a loading control (β -actin) is shown.

b. Western blot in SPCS1 and SPCS3 bulk gene-edited 293T cells. Control, SPCS1, and SPCS3 gene-edited 293T cells were infected with WNV or mock-infected for the indicated times. Lysates were Western blotted with an anti-prM human MAb (CR4293) that recognizes a shared epitope on prM and E. Higher molecular weight bands (prM- E^{hi}) likely reflect uncleaved polyprotein forms and are present only in SPCS1 and SPCS3 gene-edited 293T cells. The data is representative of two independent experiments and a loading control (β -actin) is shown.

c. Control or SPCS1^{-/-} cells were infected with WNV or left unmanipulated (- columns), and 24 h later, cell lysates were generated and probed with a polyclonal antibody against NS4B. The results are representative of two independent experiments and loading controls (β -actin) are shown.

d. Control or SPCS1^{-/-} cells were

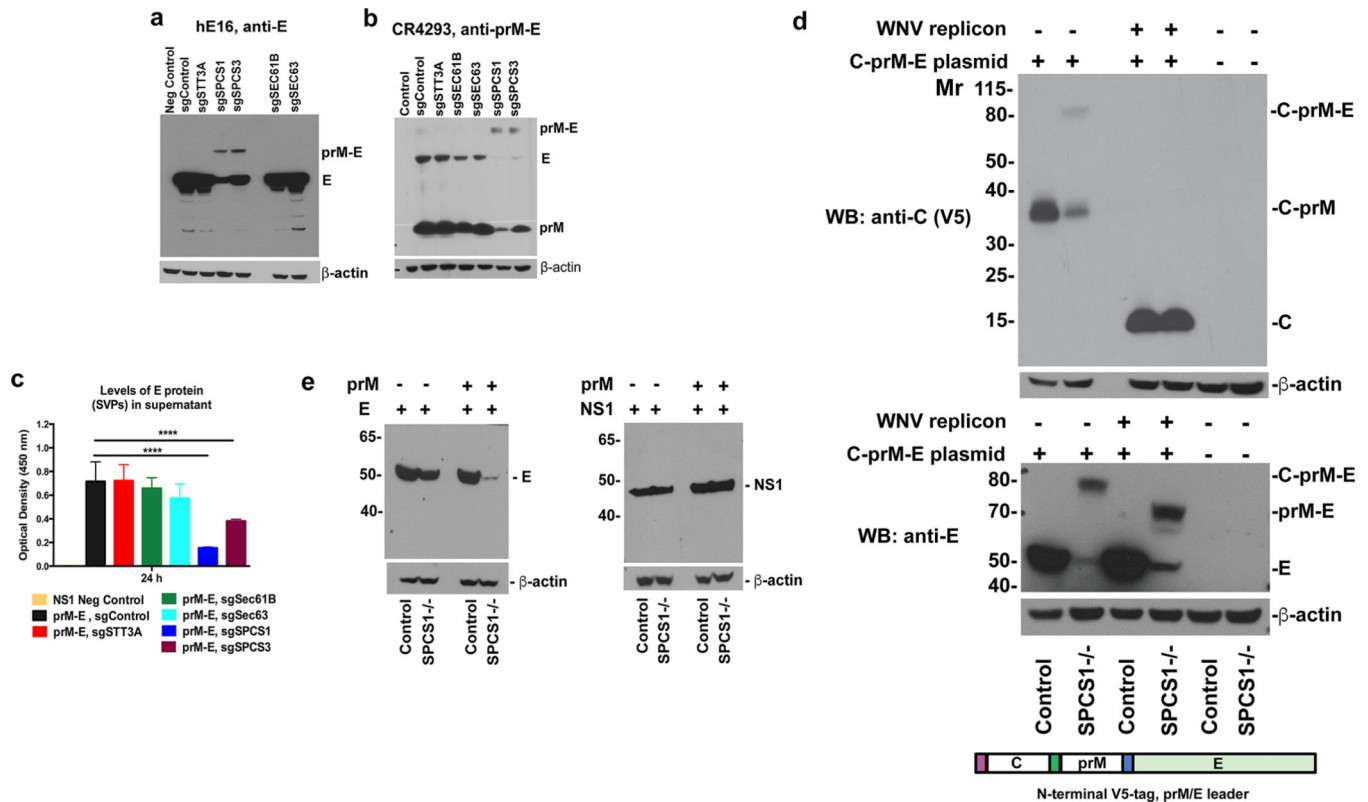
transfected with 2K-NS4B-HA plasmid. One day later, lysates were probed with an anti-HA antibody. Results are representative of two independent experiments and loading controls (β -actin) are shown. Cleaved (NS4B) and uncleaved (2K-NS4B) bands are indicated at the right of the gel. **e.** Control or SPCS1^{-/-} cells were transfected with NS1, NS1-NS2A-FLAG, or control plasmids. One day later, lysates were probed with (*left*) anti-NS1 or (*right*) anti-FLAG antibodies. Cleavage of NS1-NS2A-FLAG results in expression of the C-terminal FLAG tag exclusively with the residual NS2A protein. The results are representative of three independent experiments and loading controls (β -actin) are shown. Note, expression of NS1-NS2A results in two forms of NS1 (NS1 and NS1') due to a ribosomal frameshift event that occurs at a heptanucleotide motif located near the beginning of the NS2A gene. **f.** Control or SPCS1^{-/-} cells were infected with WNV or left unmanipulated and 24 h later, cell lysates were generated and probed with a monoclonal antibody against NS3. The results are representative of two independent experiments and loading controls (β -actin) are shown. For gel source data, see Supplementary Figure 1.



Extended Data Figure 7. Western blotting of HCV E2 in control and SPCS1 gene-edited Huh7.5 cells

Control or SPCS1 gene-edited cells were infected with HCV (MOI of 5) (+) or left untreated (-) and 48 or 72 h later, cell lysates were generated and probed with a mouse MAb against

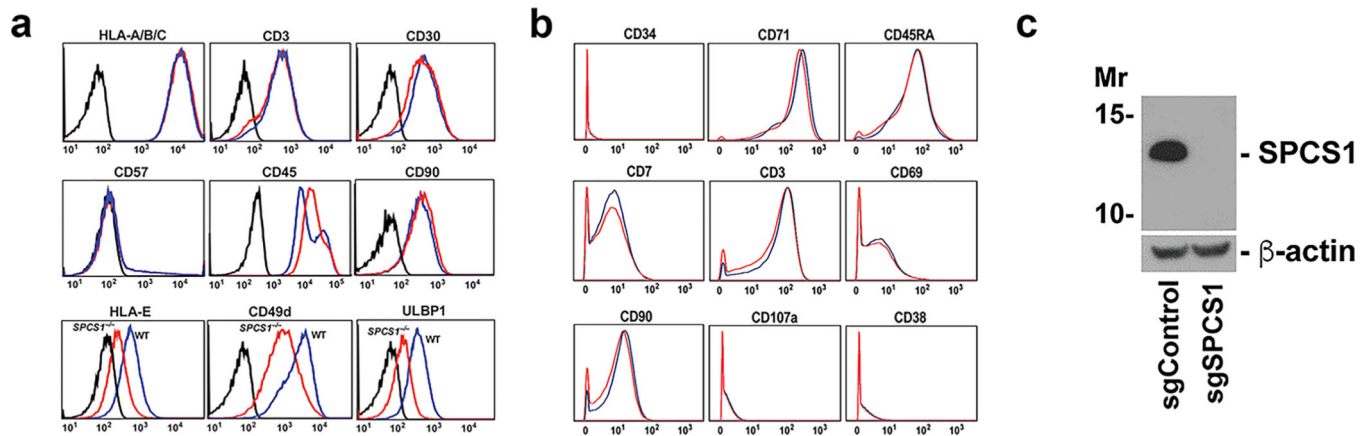
HCV E2 protein. The results are representative of two independent experiments and a normal and over-exposed blot are shown. For gel source data, see Supplementary Figure 1.



Extended Data Figure 8. Effect of sgRNA on WNV structural protein processing and production

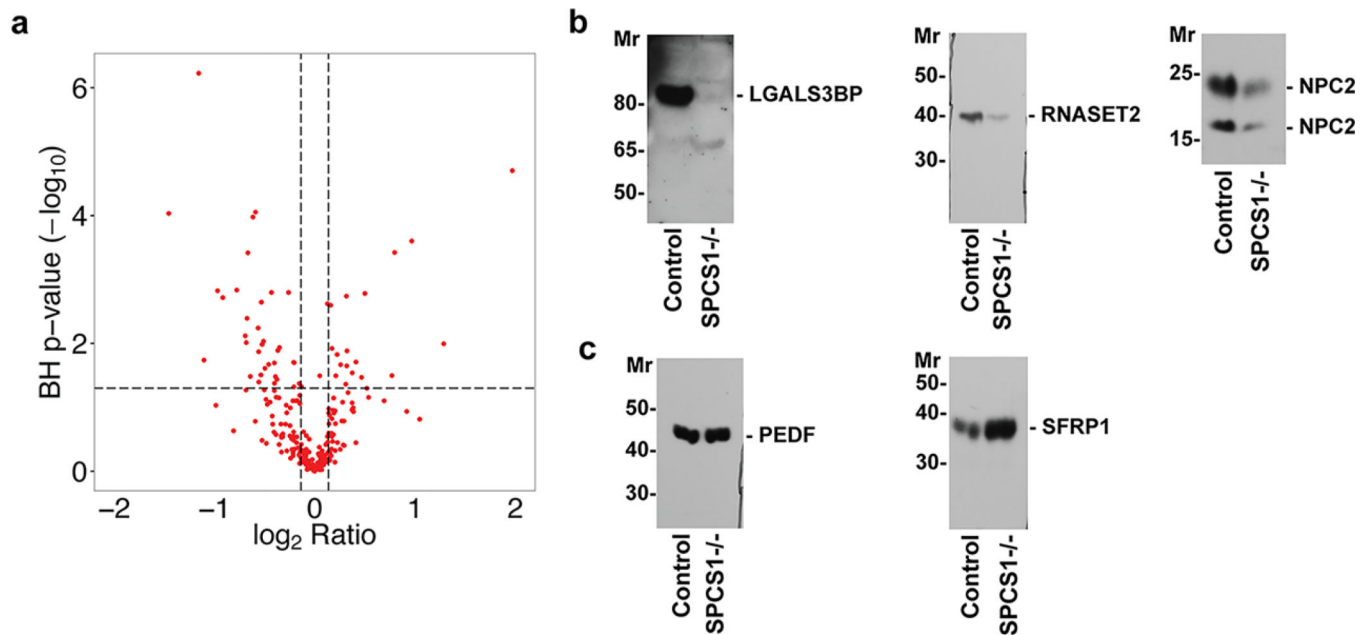
a–c. The indicated gene-edited 293T cells were transfected with a plasmid encoding WNV prM-E and subjected to Western blotting with hE16 (anti-E) (**a**) or CR4293 (anti-prM-E) (**b**). Note, the shift of the prM-E bands to high molecular weight in bulk gene-edited cells with reduced expression of SPCS1 or SPCS3. The results are representative of three independent experiments and a loading control (β -actin) is shown. **c.** 293T cells expressing the indicated sgRNA were transfected with a plasmid encoding the prM-E genes. 24 h later, supernatants were harvested and SVPs were quantitated by a capture ELISA. The results are the average of several independent experiments performed in triplicate. The asterisks indicate SVP levels in the supernatant that are statistically different compared to control cells (****, $P < 0.001$, ANOVA with a multiple comparison correction). **d.** Control or SPCS1^{-/-} clonal 293T cells were transfected with a single C-prM-E plasmid containing an N-terminal V5 tag fused to C (purple box) and native C-prM (green box) and prM-E (blue box) leader sequences. In some experiments, a cDNA launched WNV replicon was co-transfected to facilitate the cleavage of C from prM by the viral NS2B-NS3 protease. Lysates were prepared 24 h later and probed with an anti-V5 (top) or anti-E (bottom) antibody. Note, two separate gels were run for blotting with anti-V5 (C) and anti-E. One representative experiment of two is shown and a loading control (β -actin) for the top (anti-V5) gel is included. **e.** Control and SPCS1^{-/-} 293T cells were transfected with E or NS1 with or without prM co-transfection. One day after transfections, cells were harvested and lysates

were Western blotted with antibodies against E (*left*) or NS1 (*right*). Molecular weight markers and specific proteins are indicated to the left and right of each gel, respectively. The results are representative of three independent experiments. For gel source data, see Supplementary Figure 1.



Extended Data Figure 9. Expression of immune system antigens on the surface of SPCS1 gene-edited cells

a–b. Control and SPCS1 gene-edited Jurkat cells were incubated with MAbs against the indicated cell surface antigens. After washing, cells were fixed with paraformaldehyde and then processed by (a) flow cytometry or (b) mass cytometry. The histograms are as follows: Black, isotype control in WT cells; Blue, control cells; and Red, SPCS1 gene-edited cells. Results are representative of three independent experiments for flow cytometry and one run on a mass cytometer in triplicate. (c) Western blotting of bulk-selected Jurkat cells (control and SPCS1 sgRNA selected) for expression of SPCS1 (~12 kDa). For gel source data, see Supplementary Figure 1.



Extended Data Figure 10. Secretome analysis in control and SPCS1^{-/-} cell supernatants

a. Volcano plot from one-way ANOVA for secreted protein abundances between control and SPCS1^{-/-} 293T cells. The areas of dots are proportional to the \log_2 standard deviation of protein ratios. The vertical dashed lines delimit fold changes = ± 1.1 and the horizontal dashed line delimits P value = 0.05. The red dots show secreted proteins using the SP_PIR classification. Values $< \log_2$ of 0 indicate secreted proteins that show reduced expression in and SPCS1^{-/-} 293T cells. **b–c.** Western blotting of supernatants from control and SPCS1^{-/-} 293T cells. **(b)** Proteins (LGALS3BP, RNASET2, and NPC2) identified as down-regulated in SPCS1^{-/-} 293T cells by mass spectrometry (see Supplementary Tables 4 and 5). **(c)** Proteins identified as having similar or possibly higher levels in supernatants of SPCS1^{-/-} 293T cells. For gel source data, see Supplementary Figure 1.

Supplementary Material

Refer to Web version on PubMed Central for supplementary material.

Acknowledgments

NIH grants U19 AI083019 (M.S.D.), R01 AI104972 (M.S.D.), and T32 AI007163 (E.F.) supported this work. Additionally, this work was supported by the Washington University Institute of Clinical and Translational Sciences (UL1 TR000448 from the National Center for Advancing Translational Sciences and P41 GM103422-35 from the National Institute of General Medical Sciences). T.C.P and K.A.D are supported by the intramural program of NIAID. The authors wish to thank Richard Kuhn, Adolfo Garcia-Sastre, Haiyong Zhao, Daved Fremont, Xiaoli Wang, and Reid Townsend for their generosity with reagents, experimental advice, and data analysis. We also acknowledge Petra Erdmann-Gilmore, Rose Connors, Yiling Mi, and Hueylie Lin at the Washington University Proteomics Core Laboratory for expert technical assistance. Finally, we thank Xavier de Lamballerie (Emergence des Pathologies Virales, Aix-Marseille Université, Marseille, France) and the European Virus Archive goes Global (EVAg) for consenting to the use of H/PF/2013 ZIKV strain for this study under a material transfer agreement with the EVAg partner, Aix-Marseille Université.

ALL REFERENCES

1. Diamond MS, Pierson TC. Molecular Insight into Dengue Virus Pathogenesis and Its Implications for Disease Control. *Cell*. 2015; 162:488–492. [pii]. [PubMed: 26232221]
2. Weaver SC, et al. Zika virus: History, emergence, biology, and prospects for control. *Antiviral Res*. 2016; 130:69–80. [PubMed: 26996139]
3. Cong L, et al. Multiplex genome engineering using CRISPR/Cas systems. *Science*. 2013; 339:819–823. [pii]. [PubMed: 23287718]
4. Jinek M, et al. RNA-programmed genome editing in human cells. *eLife*. 2013; 2:e00471. [pii]. [PubMed: 23386978]
5. Shalem O, et al. Genome-scale CRISPR-Cas9 knockout screening in human cells. *Science*. 2014; 343:84–87. [pii]. [PubMed: 24336571]
6. Koike-Yusa H, Li Y, Tan EP, Velasco-Herrera Mdel C, Yusa K. Genome-wide recessive genetic screening in mammalian cells with a lentiviral CRISPR-guide RNA library. *Nat Biotechnol*. 2014; 32:267–273. [PubMed: 24535568]
7. Wang T, Wei JJ, Sabatini DM, Lander ES. Genetic screens in human cells using the CRISPR-Cas9 system. *Science*. 2014; 343:80–84. [PubMed: 24336569]
8. Li W, et al. MAGeCK enables robust identification of essential genes from genome-scale CRISPR/Cas9 knockout screens. *Genome Biol*. 2014; 15:554. doi:s13059-014-0554-4 [pii] 10.1186/s13059-014-0554-4. [PubMed: 25476604]
9. Evans EA, Gilmore R, Blobel G. Purification of microsomal signal peptidase as a complex. *Proc Natl Acad Sci U S A*. 1986; 83:581–585. [PubMed: 3511473]
10. Meyer HA, Hartmann E. The yeast SPC22/23 homolog Spc3p is essential for signal peptidase activity. *J Biol Chem*. 1997; 272:13159–13164. [PubMed: 9148931]
11. Khromykh AA, Kenney MT, Westaway EG. trans-Complementation of flavivirus RNA polymerase gene NS5 by using Kunjin virus replicon-expressing BHK cells. *J Virol*. 1998; 72:7270–7279. [PubMed: 9696822]
12. Jones CT, Patkar CG, Kuhn RJ. Construction and applications of yellow fever virus replicons. *Virology*. 2005; 331:247–259. [PubMed: 15629769]
13. Lindenbach, BD.; Murray, CL.; Thiel, HJ.; Rice, CM. *Fields Virology*. Knipe, DM.; Howley, PM., editors. Vol. 1. Lippincott Williams & Wilkins; 2013. p. 712-746.
14. Chambers TJ, Grakoui A, Rice CM. Processing of the yellow fever virus nonstructural polyprotein: a catalytically active NS3 proteinase domain and NS2B are required for cleavages at dibasic sites. *J Virol*. 1991; 65:6042–6050. [PubMed: 1833562]
15. Falgout B, Pethel M, Zhang YM, Lai CJ. Both nonstructural proteins NS2B and NS3 are required for the proteolytic processing of dengue virus nonstructural proteins. *J Virol*. 1991; 65:2467–2475. [PubMed: 2016768]
16. Throsby M, et al. Isolation and characterization of human monoclonal antibodies from individuals infected with West Nile Virus. *J Virol*. 2006; 80:6982–6992. [PubMed: 16809304]
17. Barth BU, Wahlberg JM, Garoff H. The oligomerization reaction of the Semliki Forest virus membrane protein subunits. *J Cell Biol*. 1995; 128:283–291. [PubMed: 7844143]
18. Lober C, Anheier B, Lindow S, Klenk HD, Feldmann H. The Hantaan virus glycoprotein precursor is cleaved at the conserved pentapeptide WAASA. *Virology*. 2001; 289:224–229. [PubMed: 11689045]
19. Schlich J, et al. Recombinant subviral particles from tick-borne encephalitis virus are fusogenic and provide a model system for studying flavivirus envelope glycoprotein functions. *J Virol*. 1996; 70:4549–4557. [PubMed: 8676481]
20. Lorenz IC, Allison SL, Heinz FX, Helenius A. Folding and dimerization of tick-borne encephalitis virus envelope proteins prM and E in the endoplasmic reticulum. *J Virol*. 2002; 76:5480–5491. [PubMed: 11991976]
21. Hanna SL, et al. N-linked glycosylation of west nile virus envelope proteins influences particle assembly and infectivity. *J Virol*. 2005; 79:13262–13274. [PubMed: 16227249]

22. Gowen BG, et al. A forward genetic screen reveals novel independent regulators of ULBP1, an activating ligand for natural killer cells. *Elife*. 2015; 4
23. Suzuki R, et al. Signal peptidase complex subunit 1 participates in the assembly of hepatitis C virus through an interaction with E2 and NS2. *PLoS Pathog*. 2013; 9:e1003589. [pii]. [PubMed: 24009510]
24. Ma H, et al. A CRISPR-Based Screen Identifies Genes Essential for West-Nile-Virus-Induced Cell Death. *Cell Rep*. 2015; 12:673–683. doi:S2211-1247(15)00675-0 [pii] 10.1016/j.celrep.2015.06.049. [PubMed: 26190106]
25. Krishnan MN, et al. RNA interference screen for human genes associated with West Nile virus infection. *Nature*. 2008; 455:242–245. [PubMed: 18690214]
26. Yasunaga A, et al. Genome-Wide RNAi Screen Identifies Broadly-Acting Host Factors That Inhibit Arbovirus Infection. *PLoS Pathog*. 2014; 10:e1003914. [pii]. [PubMed: 24550726]
27. Sessions OM, et al. Discovery of insect and human dengue virus host factors. *Nature*. 2009; 458:1047–1050. [PubMed: 19396146]
28. Rose PP, et al. Natural resistance-associated macrophage protein is a cellular receptor for sindbis virus in both insect and mammalian hosts. *Cell Host Microbe*. 2011; 10:97–104. [pii]. [PubMed: 21843867]
29. Brien JD, Lazear HM, Diamond MS. Propagation, quantification, detection, and storage of West Nile virus. *Curr Protoc Microbiol*. 2013; 31:15D 13 11–15D 13 18.
30. Jiang J, Luo G. Cell culture-adaptive mutations promote viral protein-protein interactions and morphogenesis of infectious hepatitis C virus. *J Virol*. 2012; 86:8987–8997. [PubMed: 22674987]
31. Sabo MC, et al. Neutralizing Monoclonal Antibodies against Hepatitis C Virus E2 Protein Bind Discontinuous Epitopes and Inhibit Infection at a Postattachment Step. *J Virol*. 2011; 85:7005–7019. doi:JVI.00586-11 [pii] 10.1128/JVI.00586-11. [PubMed: 21543495]
32. Sanjana NE, Shalem O, Zhang F. Improved vectors and genome-wide libraries for CRISPR screening. *Nat Methods*. 2014; 11:783–784. [pii]. [PubMed: 25075903]
33. Oliphant T, et al. Development of a humanized monoclonal antibody with therapeutic potential against West Nile virus. *Nature Medicine*. 2005; 11:522–530.
34. Oliphant T, et al. Antibody recognition and neutralization determinants on domains I and II of West Nile Virus envelope protein. *J Virol*. 2006; 80:12149–12159. [PubMed: 17035317]
35. Pal P, et al. Development of a highly protective combination monoclonal antibody therapy against Chikungunya virus. *PLoS Pathog*. 2013; 9:e1003312. [PubMed: 23637602]
36. Fuchs A, Pinto AK, Schwaeble WJ, Diamond MS. The lectin pathway of complement activation contributes to protection from West Nile virus infection. *Virology*. 2011; 412:101–109. doi:S0042-6822(11)00008-0 [pii] 10.1016/j.virol.2011.01.003. [PubMed: 21269656]
37. Boutros M, et al. Genome-wide RNAi analysis of growth and viability in *Drosophila* cells. *Science*. 2004; 303:832–835. [pii]. [PubMed: 14764878]
38. Hackett BA, et al. RNASEK is required for internalization of diverse acid-dependent viruses. *Proc Natl Acad Sci U S A*. 2015; 112:7797–7802. [pii]. [PubMed: 26056282]
39. Lin TY, et al. A novel approach for the rapid mutagenesis and directed evolution of the structural genes of west nile virus. *J Virol*. 2012; 86:3501–3512. doi:JVI.06435-11 [pii] 10.1128/JVI.06435-11. [PubMed: 22258236]
40. Pierson TC, et al. A rapid and quantitative assay for measuring antibody-mediated neutralization of West Nile virus. *Virology*. 2006; 346:53–65. [PubMed: 16325883]
41. Mishin VP, Cominelli F, Yamshchikov VF. A 'minimal' approach in design of flavivirus infectious DNA. *Virus Res*. 2001; 81:113–123. doi:S0168170201003719 [pii]. [PubMed: 11682130]
42. Chung KM, et al. Antibodies against West Nile virus non-structural (NS)-1 protein prevent lethal infection through Fc gamma receptor-dependent and independent mechanisms. *J Virol*. 2006; 80:1340–1351. [PubMed: 16415011]
43. Beasley DW, et al. Envelope protein glycosylation status influences mouse neuroinvasion phenotype of genetic lineage 1 West Nile virus strains. *J Virol*. 2005; 79:8339–8347. [PubMed: 15956579]

44. Munoz-Jordan JL, et al. Inhibition of alpha/beta interferon signaling by the NS4B protein of flaviviruses. *J Virol.* 2005; 79:8004–8013. [PubMed: 15956546]
45. Medigeshi GR, et al. West Nile virus infection activates the unfolded protein response leading to CHOP induction and apoptosis. *J Virol.* 2007
46. Miner JJ, et al. Cytoplasmic domain of P-selectin glycoprotein ligand-1 facilitates dimerization and export from the endoplasmic reticulum. *J Biol Chem.* 2011; 286:9577–9586. [PubMed: 21220419]
47. Kall L, Canterbury JD, Weston J, Noble WS, MacCoss MJ. Semi-supervised learning for peptide identification from shotgun proteomics datasets. *Nat Methods.* 2007; 4:923–925. [PubMed: 17952086]
48. Huang da W, Sherman BT, Lempicki RA. Systematic and integrative analysis of large gene lists using DAVID bioinformatics resources. *Nat Protoc.* 2009; 4:44–57. [PubMed: 19131956]
49. Huang da W, Sherman BT, Lempicki RA. Bioinformatics enrichment tools: paths toward the comprehensive functional analysis of large gene lists. *Nucleic Acids Res.* 2009; 37:1–13. [PubMed: 19033363]

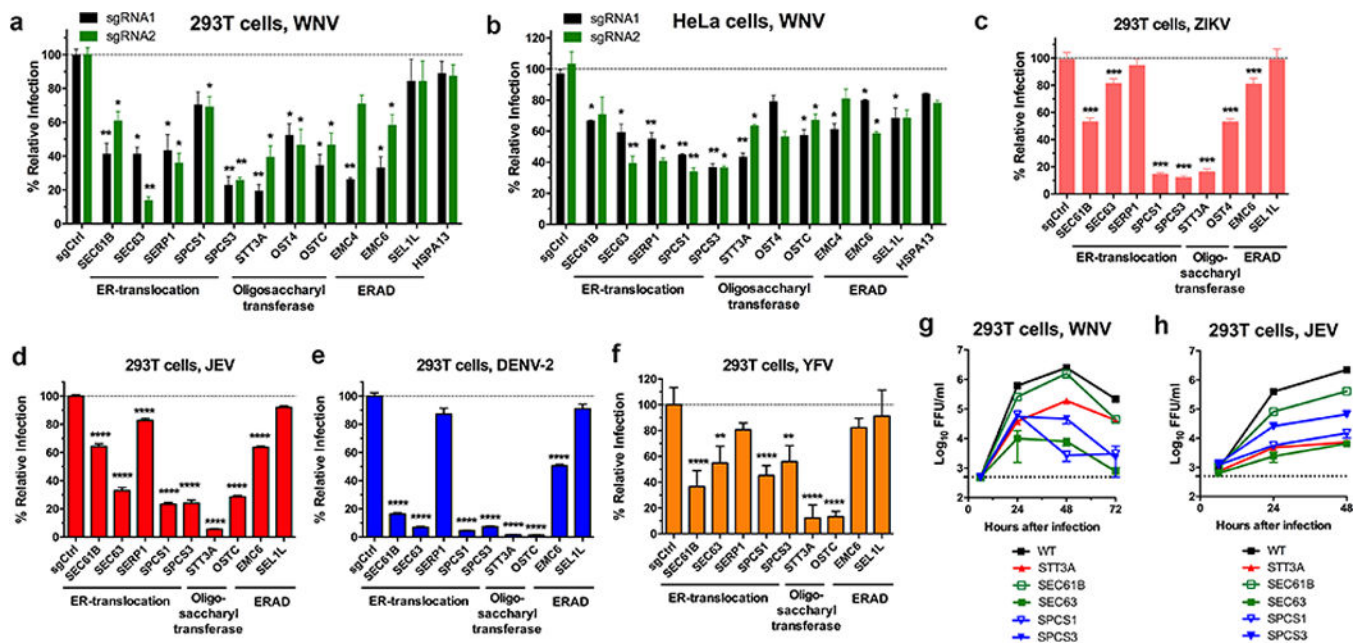


Figure 1. Genes required for flavivirus infection

a–b. Genes were selected for validation based on statistical analysis (Supplementary Tables 1 and 2). Gene-edited **(a)** 293T and **(b)** HeLa cells were infected with WNV and 12 h later analyzed for E protein. **c–f.** Effect of gene editing on **(c)** ZIKV, **(d)** JEV, **(e)** DENV, and **(f)** YFV infection in 293T cells. The results are the average of two to three independent experiments. **a–f.** Error bars indicate standard error of the means (SEM). Statistical significance was determined by an ANOVA with a multiple comparisons correction (*, $P < 0.05$; **, $P < 0.01$; ***, $P < 0.0001$). **g–h.** 293T cells expressing indicated sgRNA were infected with WNV **(g)** or JEV **(h)** and virus yield was determined. One of two independent experiments performed in triplicate is shown. Error bars indicate SEM.

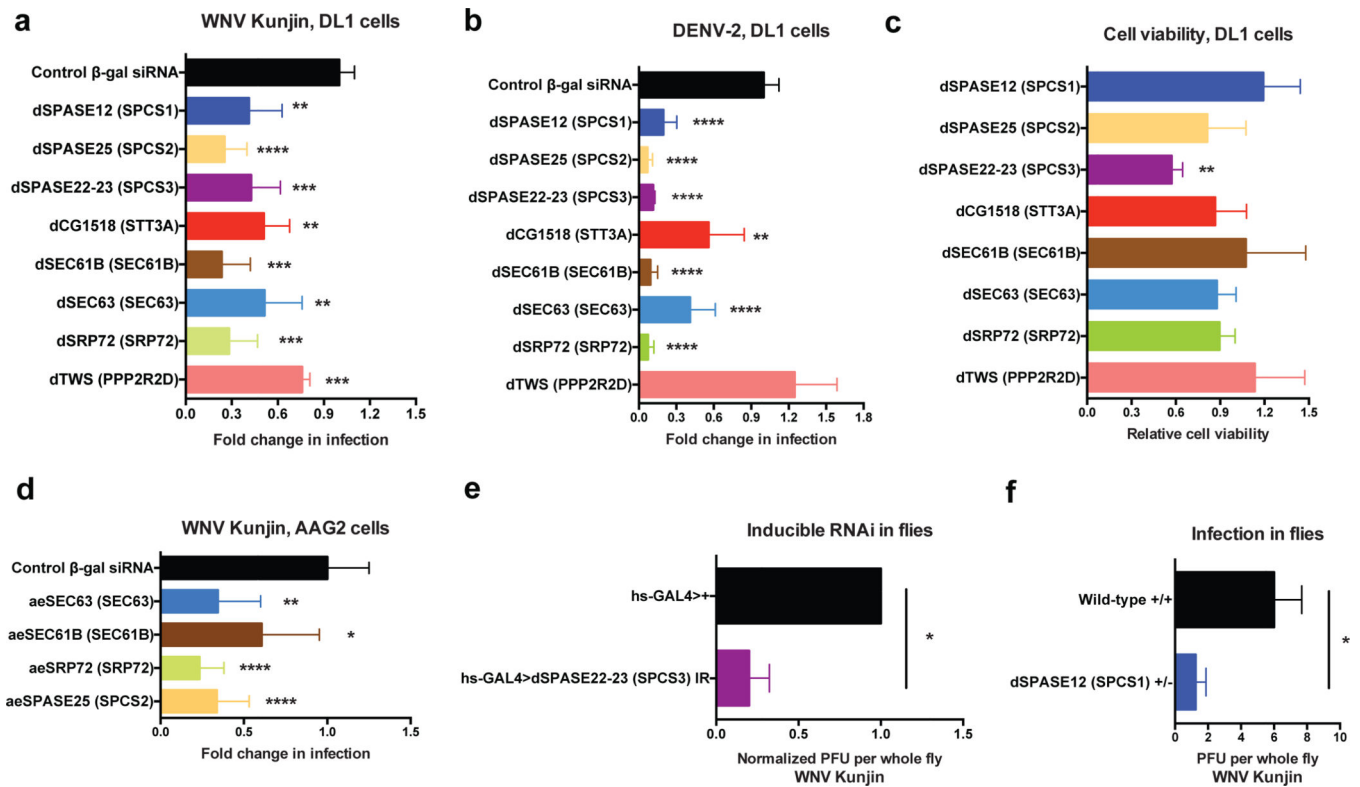


Figure 2. Requirement of ER-associated genes for flavivirus infection of insect cells

a–b. *Drosophila* DL1 cells were treated with dsRNA and infected with (a) WNV (Kunjin) or (b) DENV-2 for 30 h. The percentage of infected cells was normalized to the control β -galactosidase dsRNA. The data is expressed as the mean normalized value \pm standard deviations (SD). Statistically significant differences (**, $P < 0.01$; ***, $P < 0.001$; ****, $P < 0.0001$) compared to control dsRNA are indicated. The data is pooled from four experiments in duplicate. **c.** Cell viability. DL1 cells were treated with dsRNA and 30 h later processed. **d.** *Aedes aegypti* AAG2 cells were treated with dsRNA, infected with WNV (Kunjin) for 30 h, and processed for viral antigen. **e.** dSPCS1 silenced flies (Hs-Gal4 > UAS-dSPASE22-23 [SPCS3] IR) or sibling controls were infected with WNV (Kunjin) and titers measured 7 days later. The fold-change in titer of pools of ten flies from three experiments is shown (normalized mean \pm SD, * $P < 0.05$). **f.** WT (+/+) or Spase12(EY10774) heterozygous (+/-) sibling flies were infected with WNV (Kunjin) and titers measured 7 days later. Data from pools of five flies in three independent experiments is shown (*, $P < 0.05$ by Student's t test).

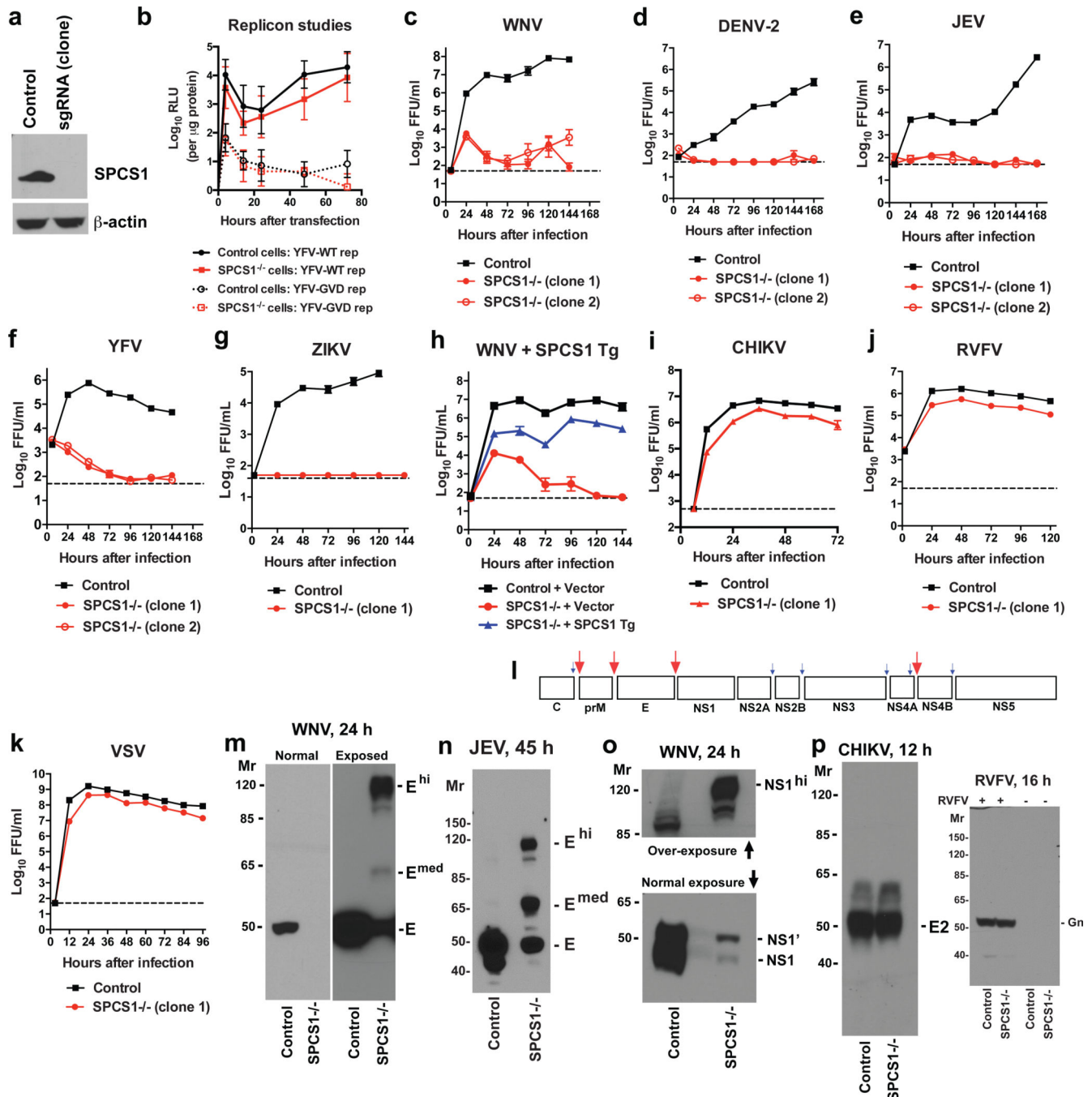


Figure 3. SPCS1 is required for flavivirus protein processing and infection

a. Western blotting of SPCS1^{-/-} 293T cells. **b.** Cells were transfected with YFV-luciferase replicon RNA (WT GDD or loss-of-function GVD). Firefly luciferase activity was measured and normalized to intracellular protein levels. The data reflects the average of two to three independent experiments performed in duplicate. **c–h.** Cells were infected with WNV (**c**, **h**), DENV-2 (**d**), JEV (**e**), YFV (**f**) or ZIKV (**g**), and viral yield measured. In **h**, cells were trans-complemented with an SPCS1 or control plasmid. Results are the average of two to three independent experiments performed in triplicate. **i–k.** Cells were infected with CHIKV

(alphavirus), RVFV (bunyavirus), or VSV (rhabdovirus) and viral yield was measured. Results are the average of two to three independent experiments performed in triplicate. **l**. The polyprotein processing strategy of flaviviruses¹³. Red and blue arrows indicate sites of cleavage by host and viral (NS2B-NS3) proteases, respectively. **m–o**. Control or SPCS1^{-/-} 293T (**m**, **o**) or Huh7.5 (**n**) cells were infected with WNV (**m**, **o**) or JEV (**n**). Lysates were blotted with (**m**) anti-WNV E, (**n**) anti-JEV E, or (**o**) anti-WNV NS1 MAbs. Higher molecular weight bands (E^{hi}, E^{med}, and NS1^{hi}) that react with anti-flavivirus MAbs are indicated. One experiment of three is shown. **p**. 293T cells were infected with CHIKV or RVFV. Lysates were blotted with anti-CHIKV E2 or anti-RVFV Gn mAbs. One experiment of two is shown. For gel source data, see Supplementary Figure 1.

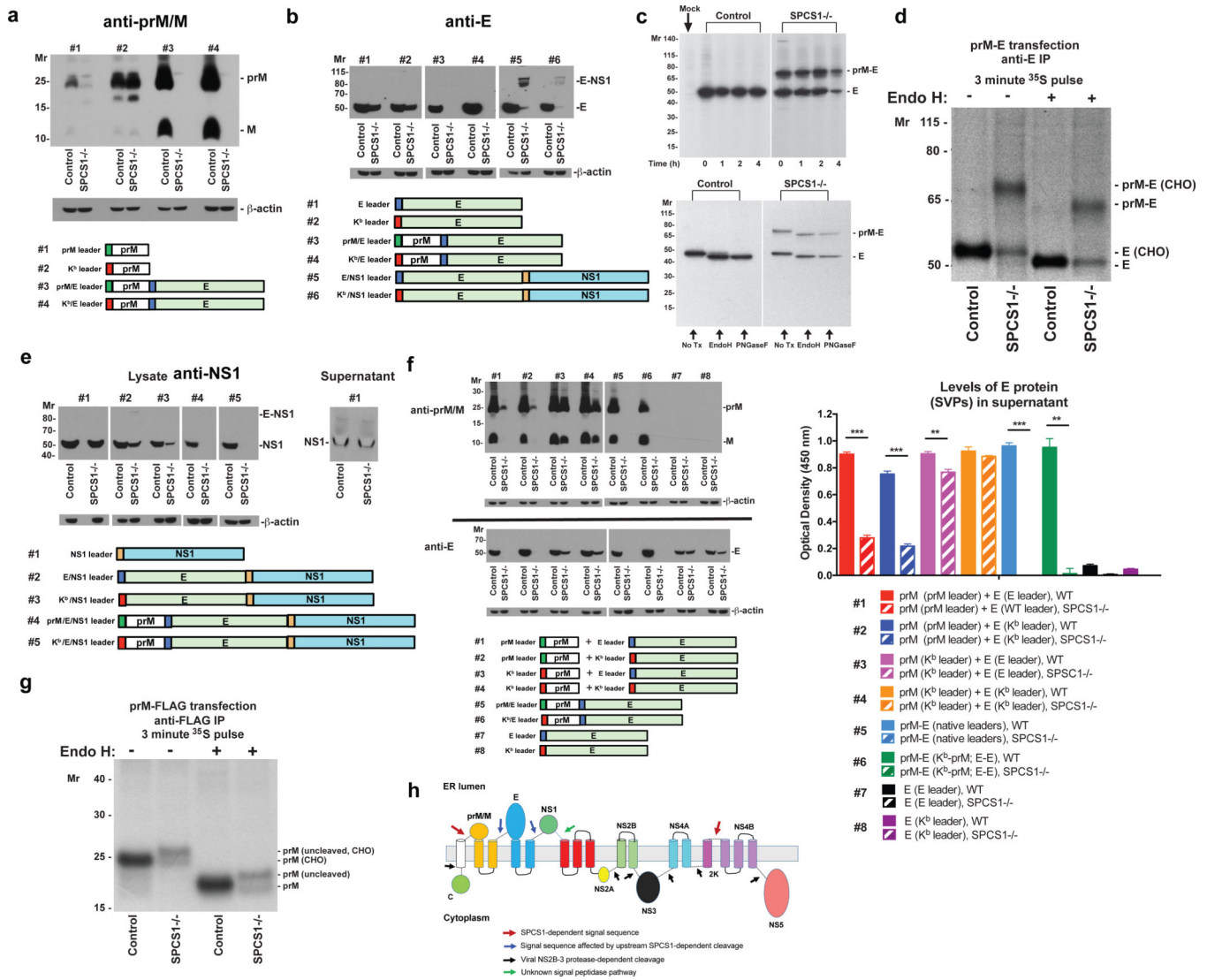


Figure 4. SPCS1 is required for cleavage of the C-prM leader peptide and internal leader sequences

a. 293T cells were transfected with prM or prM-E plasmids containing native (C-prM (green box) and prM-E (blue box) leader sequences) or K^b (red box) leader sequences. Blots of lysates were probed with anti-prM/M mAb. One experiment of three is shown. **b.** 293T cells were transfected with E, prM-E, and E-NS1 plasmids containing native leader sequences (described in **(a)** and E-NS1 (orange box)) or a K^b leader. Blots of lysates were probed with anti-E mAb. A higher molecular weight band corresponds to uncleaved E-NS1. One experiment of two is shown. **c-d.** 293T cells were transfected with a prM-E plasmid. 24 h later, cells were labeled for 40 (**c**) or 3 (**d**) min with ³⁵S cysteine-methionine. Lysates were immunoprecipitated with an anti-E protein MAb prior to SDS-PAGE. (**c** (Top)) Cysteine-methionine was added for chase times (0 to 4 h). (**c** (Bottom) and **d**) Immunoprecipitates were untreated or treated with Endo H or PNGase F for 1 h at 37°C. One experiment of two is shown. **e.** 293T cells were transfected with NS1, E-NS1, and prM-E-NS1 plasmids containing native viral or K^b leaders. Blots of lysates or supernatants were probed with anti-

NS1 mAb. One experiment of two is shown. **f.** 293T cells were transfected with prM + E, prM-E, or E plasmids containing viral or K^b leaders. (*Left*) Blots of lysates were probed with anti-prM/M or anti-E MAbs. One experiment of two is shown. (*Right*) Levels of SVPs in supernatant at 24 h. Data are pooled from independent experiments performed in triplicate (**, $P < 0.01$; ***, $P < 0.001$; ****, $P < 0.0001$, unpaired t test). **g.** 293T cells were transfected with prM-FLAG. 24 h later, cells were labeled for 3 min with ³⁵S cysteine-methionine. Lysates were immunoprecipitated with anti-FLAG protein mAb. **h.** Model of processing of flavivirus structural and non-structural proteins based on infection and transfection studies and the literature^{14,15}. Arrows indicate cleavage sites requiring SPCS1, sites affected by upstream SPCS1-dependent events, sites cleaved by the viral NS2B-NS3 protease, and sites cleaved via an SPCS1-independent pathway. For gel source data, see Supplementary Figure 1.